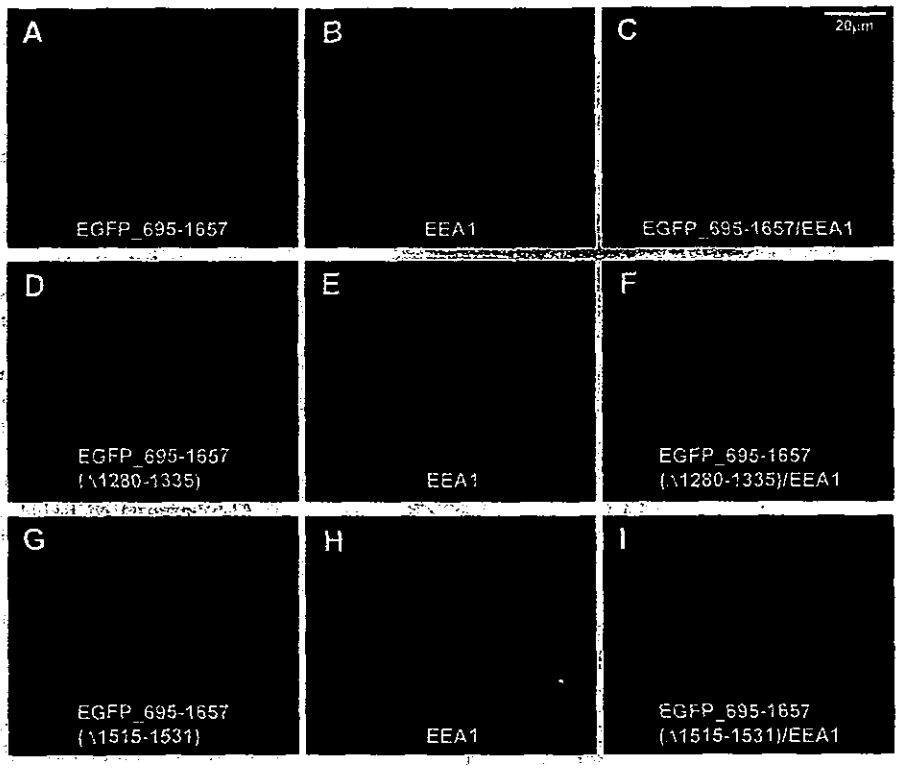


FIG. 6. **A constitutive active form of ALS2 (EGFP_695–1657) induces the enlargement of the EEA1-positive compartments in a Rab5GEF/oligomerization-dependent fashion.** HeLa cells were transfected with pEGFP-ALS2_695–1657 (*A–C*), pEGFP-ALS2_695–1657 (Δ1280–1335) (*D–F*), or pEGFP-ALS2_695–1657 (Δ1515–1531) (*G–I*). Forty-eight hours after transfection, HeLa cells were labeled with anti-EEA1 antibody. The fluorescence of EGFP-ALS2 (*A*, *D*, and *G*) and Alexa-594 secondary antibody (*B*, *E*, and *H*) was detected and visualized by confocal microscopy. *Yellow stainings* in the *merged images* (*right*; *C*, *F*, and *I*) represent the overlapping signals between two different images (*left* and *middle*).

homo-oligomerized (data not shown). As shown in Fig. 6*A*, expression of EGFP_695–1657 resulted in enlarged endosomes and most of them were EEA1-positive vesicles (Fig. 6*C*), implying that EGFP_695–1657 enlarges early endosomes. Next, we evaluated the effect of the oligomerization-defective/Rab5GEF-defective ALS2 mutant, EGFP_695–1657 (Δ1280–1335), on the endosome phenotypes in HeLa cells. Notably, results showed that this mutation completely abolished the capabilities of the early endosome enlargement. Furthermore, this mutant ALS2 peptide also localized onto the vesicular structures (Fig. 6*D*), representing the EEA1-negative (Fig. 6, *D–F*) and Rab5A-negative compartments (data not shown). Overexpression of the EGFP_695–1657 (Δ1515–1531) oligomerization-prone/Rab5GEF-defective mutant also demonstrated that this mutant lost its ability to induce the endosome enlargement, consistent with our previous results using two VPS9-domain mutants, EGFP_660–1657 (P1603A) and EGFP_660–1657 (L1617A) (30). Collectively, these results indicate that the oligomerization of ALS2 requisite for the Rab5GEF activity is indeed crucial for the endosome enlargement induced by overexpression of constitute active forms of ALS2 in the cells, and that, in particular, the Rab5GEF activity associated with ALS2 might be an essential feature for the ALS2-associated physiological function on endosome trafficking.

## DISCUSSION

We have previously demonstrated that the ALS2 protein is involved in endosomal dynamics through its intrinsic Rab5GEF activity mediated by the C-terminal MORN/VPS9 domains (30). In this study, we show for the first time that ALS2 forms a homo-oligomeric complex through its C-terminal region and that this oligomerization is essential for the ALS2-associated Rab5GEF activity and its regulatory function on endosome dynamics, such as endosome enlargement.

Our co-immunoprecipitation and gel filtration analyses revealed that the ectopically expressed FLAG-tagged ALS2 protein formed a very stable oligomer, presumably an octamer in the cells. Self-interaction was also detected when either the HA-tagged or EGFP-fused form of ALS2 was used (data not shown). Furthermore, untagged or even endogenous ALS2 was immunoprecipitated with epitope-tagged truncated ALS2 peptide carrying the C-terminal region (data not shown). These results strongly suggest that the endogenous ALS2 protein exists as an oligomeric form *in vivo*. In this study, we also determined the regions requisite for the ALS2 homo-oligomerization by co-immunoprecipitation and Y2H using various truncated or internally deleted ALS2 fragments. The results showed that two distinct non-overlapping regions, aa 1233–1351 and 1351–1548, mediated oligomerization by interacting with each other. These two regions reside within the region flanked by MORN motifs and VPS9 domain where no known motifs and/or domains have ever been assigned. Notably, the aa 1280–1335 region must contain the crucial residues determining the structural basis for the ALS2 oligomerization, because deletion of this portion completely abolished the oligomerization. Unfortunately, we have so far failed to obtain the sufficient amounts of the oligomerization-defective ALS2 proteins, including ALS2_L (Δ1280–1335) and ALS2_1100–1657 (Δ1280–1335), due to their inefficient expression as soluble proteins in the cells, and thus could not analyze these proteins by gel-filtration as to whether they existed as monomers in the cells. Based upon our results, two structural models for the ALS2 oligomerization could be possible (Fig. 7). One is that the dimerized ALS2 units in an anti-parallel fashion may form an octamer (Fig. 7*A*), and the other could be that eight ALS2 molecules form an octagon-like structure (Fig. 7*B*). Further experiments will clarify the *bona fide* tertiary structure for the oligomerized ALS2 protein complex.

In this study, we also obtained the important insights into the functional-structural relationship by characterizing the oligomerization of ALS2 and its associated Rab5GEF activity *in vitro*. We have previously shown that the C-terminal region spanning MORN and the VPS9 domain of ALS2 consists of the

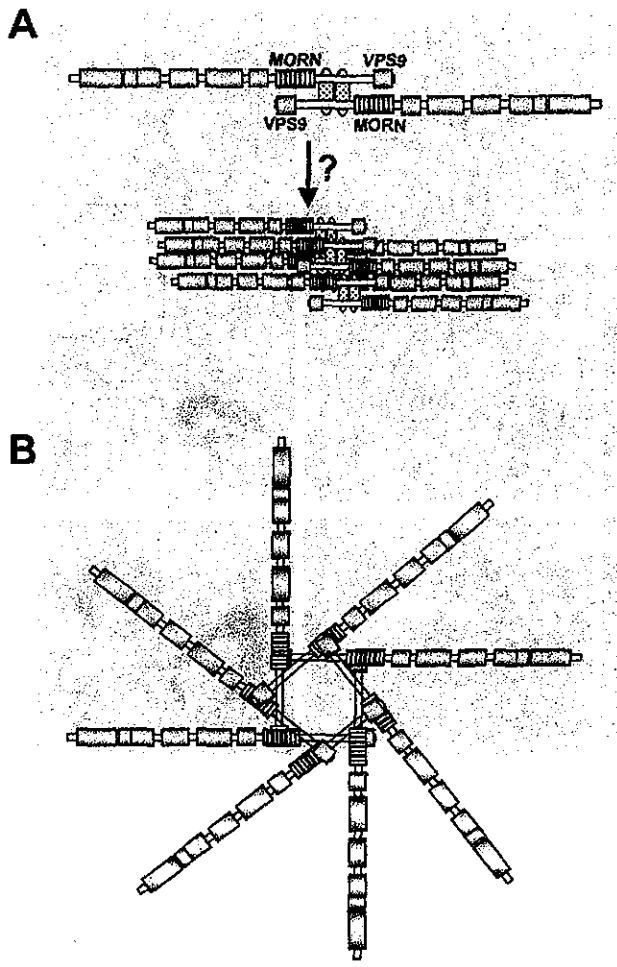


FIG. 7. **Two possible models for the ALS2 oligomeric structure.** Schematic representations of the ALS2 oligomers deduced from the present study. *A*, two ALS2 molecules that interact with each other in an anti-parallel manner (the dimer units) form oligomeric complexes by the yet to be identified mechanism. *Two dotted areas* represent the C-terminal region-mediated interaction. *B*, eight ALS2 molecules form an octagon-like structure through the C-terminal region-mediated interaction.

minimum required region for the ALS2-associated Rab5GEF activity (30). Present results in conjunction with the previous findings suggest that a number of key elements regulating the ALS2-associated Rab5GEF activity reside within the C-terminal region, including not only the MORN motifs and VPS9 domain (30) but also other regions, such as aa 1280–1335 and aa 1515–1531. Notably, one of these elements, corresponding to aa 1280–1335, was found to be the region requisite for the ALS2 oligomerization. This result indicates that the ALS2 homo-oligomerization can be one of the key determinants for the ALS2-associated Rab5GEF activity and, thus, a pivotal molecular feature underlying the physiological function for ALS2 *in vivo*. In fact, our *in vitro* GEF activity assay revealed that the oligomerization-defective ALS2 mutants completely lost their Rab5GEF activities. However, besides these oligomerization-defective mutants, all other Rab5GEF-defective ALS2 mutants still retained their ability to form the oligomers, suggesting that oligomerization itself is not sufficient to activate Rab5. Furthermore, all the normal as well as mutant ALS2 proteins examined bound to Rab5A, irrespective of whether they retained the Rab5GEF activity and/or the oligomerization capability or not, implying that ALS2·Rab5 binding is not also a sole determinant for the ALS2-associated Rab5GEF activity. Taken together, it is suggested that every element determining the structural content of the ALS2 protein complex, ALS2 oligomerization, and the formation of the ALS2·Rab5 complex, might be important for its normal Rab5GEF activity mediated by the C-terminal region of ALS2.

With regard to the minimum catalytic region for the ALS2-associated GEF activity, Topp *et al.* (31) have recently reported the contradictory result, in which the C-terminal portion of ALS2 fragment (ALS2_1360–1657 aa) lacking both MORN motifs as well as the region crucial for the oligomerization (determined in this study) possesses Rab5GEF activity *in vitro*. In our results, the oligomerization-defective/Rab5GEF-defective ALS2 protein, ALS2_695–1657 (Δ1280–1335), covering the entire ALS2_1360–1657 peptide, loses the ALS2-associated Rab5GEF activity. Although it is conceivable that this discrepancy could be a result of different assay conditions used, the answer for this question remains elusive.

Given the importance of the ALS2 self-interaction in the ALS2-associated Rab5GEF activity, ALS2 homo-oligomerization must also play significant roles on the modulation of endosome/vesicle trafficking, and thus the loss of oligomerization should exhibit significant impact on the endosomal phenotypes. Remarkably, we demonstrate here that the ALS2 mutant carrying the intact DH/PH domain but lacking one of the self-interacting regions, ALS2_695–1657 (Δ1280–1335), completely lost the normal endosomal (EEA1-positive) localization and enlarged endosome phenotypes, whereas the oligomerization-prone WT fragment (ALS2_695–1657) localized predominantly onto EEA1-positive compartments and induced the prominent enlargement. These results imply that homo-oligomerization is one of the fundamental molecular features for the ALS2 function *in vivo*. Nevertheless, it should be noted again that oligomer formation alone is not sufficient for the endosomal localization and function of ALS2, because the oligomerization-prone/Rab5GEF-defective mutant ALS2 also miss-localized in the cells. Since the oligomerization-defective ALS2 fragments, such as ALS2-695-1657 (Δ1280–1335), always exhibit no Rab5GEF activity, we cannot formally rule out the possibility that the loss of Rab5GEF activity rather than oligomerization itself resulted in the miss-localization of the ALS2_695–1657 (Δ1280–1335) protein at present.

Recently, several studies on the subcellular distribution and function of the ALS2 protein have been reported (31, 32). We have previously demonstrated the presence of regulatory elements and domains within the ALS2 molecule (30). The N-terminal RLD appears to suppress recruitment of ALS2 onto vesicles and/or endosomes, particularly in non-neuronal cells. By contrast, the DH/PH domains facilitate the endosomal localization of ALS2 and, at the same time, enhance the C-terminal MORN/VPS9 domain-mediated endosome fusions *in vivo*. Because this DH/PH-mediated enhancing effect is totally dependent on the intact Rab5GEF activity (see Fig. 6) (30), DH/PH appears to function as an upstream-regulatory element to the MORN/VPS9 domain-mediated function. In addition, the N-terminally truncated ALS2 mutant carrying the intact MORN-VPS9 region (ALS2_1018–1657), which retains both the oligomerization and full-Rab5GEF potencies, loses the prominent endosome phenotypes, indicating that the presence of DH/PH domains followed by the intact MORN/VPS9 region might be crucial for the regulation on endosome trafficking in the cells (30). Topp *et al.* (31) also presumed that DH/PH and VPS9 domains were mainly involved in the ALS2 membranous localization, consistent with our findings. Furthermore, they also reported that the DH/PH domain could directly interact with Rac1 and that overexpression of ALS2 along with Rac1 in Sf9 cells resulted in an increase in the level of GTP-bound form

of Rac1 (active Rac1) despite the fact that we and others have so far failed to show the ALS2-associated direct catalytic GEF activity on either Rac1, Cdc42, or RhoA (30, 31). These results suggest that ALS2 could indirectly activate the Rac1-mediated signaling pathway possibly through the interaction between ALS2_DH/PH and Rac1. However, it is still unclear whether the ALS2-mediated Rac1 activation contributes to the endosome dynamics. On the other hand, Yamanaka *et al.* (32) have reported a seemingly contradictory finding that endosomal localization of ALS2 is mediated through the RLD region. Recently, we found that localization of ectopically expressed ALS2 and its phenotypic effects on endosomes appeared to be different in different types of cultured cells (30). Because each study described above has utilized different types of cultured cells and conditions, the variable effect of the ALS2 domains on the subcellular localization of ALS2 observed might reflect the differences in the physiological conditions. Together, evidence has accrued to support the notion that subcellular localization and function of ALS2 are independently or cooperatively regulated by the domain-mediated protein-protein or protein-lipid interactions, which take place under a certain physiological condition.

In this study, we demonstrated the first molecular evidence for the homophilic oligomerization to be associated with Rab5GEF activity. To our knowledge, among the VPS9 domain-containing Rab5GEF family members, ALS2 is second only to RIN2, revealing its potencies to form homophilic oligomers. Saito *et al.* (19) reported that RIN2 might exist as a tetramer composed of anti-parallel linkage of two parallel dimers. However, it has yet to be determined whether tetramer formation of RIN2 is essential for its Rab5GEF activity or not. On the other hand, Rabex-5, one of the mostly characterized mammalian Rab5GEF, has been shown to interact with Rabaptin-5 (16, 33, 34). This heterophilic complex formation strongly enhanced the Rabex-5-associated Rab5GEF activity and was essentially required for the endosome fusions (35). These findings fuel speculation that the Rab5GEFs might function as a multiple protein complex *in vivo*, regardless of whether homo- or heterophilic complexes are formed. By contrast, several RhoGEFs, including β1PIX (36, 37), Dbl (38), RasGRF1 (39), RasGRF2 (39), p115RhoGEF (40, 41), LARG (41), and PDZ-RhoGEF (41), have already been shown to dimerize or oligomerize. Inhibition of oligomerization diminishes the *in vivo* GEF activity of Dbl (38) and abolishes β1PIX function *in vivo* (37). In the cases of p115RhoGEF, LARG, and PDZ-RhoGEF, deletion of the C-terminal parts that were required for oligomerization had no significant effect on the *in vitro* GEF activities but resulted in the drastic stimulation of *in vivo* functions (40, 41). Taken together, these findings suggest that oligomerization may be an important common molecular feature in the GDP/GTP exchanging reactions on the small GTPase, which are mediated by either some members of Rab5GEFs or RhoGEFs, albeit with fundamental differences in their physiological roles.

Thus far, nine independent homozygous *ALS2* mutations resulting in three distinct but clinically overlapping recessive motor neuron diseases, ALS2, PLSJ, and IAHSP/HSP, have been reported. All these mutations cause the disruption of the coding sequences, leading to the functionally defective truncated ALS2 proteins. Because a feature common to these mutations is the loss of intact VPS9 domain, dysregulation of endocytic trafficking due to the loss of the ALS2-associated Rab5GEF activity might underlie the pathogenesis for these disorders. In this study, we identified a novel alternative splicing variant that lacked the sequences encoded by entire exon 25. This novel variant is predicted to produce internally deleted ALS2 protein (aa Δ1280–1335), which is oligomerization- and Rab5GEF-defective. At the moment, the abundance of this variant is undetermined, and thus its biological relevance is also unclear. However, it is conceivable that this oligomerization-defective ALS2 could diminish the function of ALS2 by sequestering certain important ALS2 interactors *in vivo*, thereby being implicated in the dysregulation of normal endosome dynamics.

In summary, here we show that the ALS2 oligomerization is crucial for the ALS2-mediated modulation of endosome dynamics. These findings are an important step to fully understand the ALS2 functions on endosomal dynamics. In addition to such endosome-related ALS2 function, a recent study has also revealed that ALS2 protects the cultured neuronal cells from toxicity induced by mutated Cu/Zn-superoxide dismutase (42), suggesting the possible neuroprotective function for ALS2. Further studies on the normal function for ALS2 will give us more insight toward the comprehension of pathogenesis underlying a number of recessive motor neuron disease caused by loss of functional mutation in the *ALS2* gene.

*Acknowledgments*—We are grateful to all the members of our laboratory for helpful discussion and suggestions.

REFERENCES

1. Hadano, S., Hand, C. K., Osuga, H., Yanagisawa, Y., Otomo, A., Devon, R. S., Miyamoto, N., Showguchi-Miyata, J., Okada, Y., Singaraja, R., Figlewicz, D. A., Kwiatkowski, T., Hosler, B. A., Sagie, T., Skaug, J., Nasir, J., Brown, R. H., Jr., Scherer, S. W., Rouleau, G. A., Hayden, M. R., and Ikeda, J.-E. (2001) *Nat. Genet.* **29,** 166–173
2. Yang, Y., Hentati, A., Deng, H. X., Dabbagh, O., Sasaki, T., Hirano, M., Hung, W. Y., Ouahchi, K., Yan, J., Azim, A. C., Cole, N., Gascon, G., Yagmour, A., Ben-Hamida, M., Pericak-Vance, M., Hentati, F., and Siddique, T. (2001) *Nat. Genet.* **29,** 160–165
3. Ben Hamida, M., Hentati, F., and Ben Hamida, C. (1990) *Brain* **113,** 347–363
4. Lerman-Sagie, T., Filiano, J., Smith, D. W., and Korson, M. (1996) *J. Child. Neurol.* **11,** 54–57
5. Eymard-Pierre, E., Lesca, G., Dollet, G., Santorelli, F. M., di Capua, M., Bertini, E., and Boespflug-Tanguy, O. (2002) *Am. J. Hum. Genet.* **71,** 518–527
6. Lesca, G., Eymard-Pierre, E., Santorelli, F. M., Cusmai, R., di Capupa, M., Valente, E. M., Attia-Sobol, J., Plauchu, H., Leuzzi, V., Ponzone, A., Boespflug-Tanguy, O., and Bertini, E. (2003) *Neurology* **60,** 674–682
7. Devon, R. S., Helm, J. R., Roulean, G. A., Leitner, Y., Lerman-Sagie, T., Lev, D., and Hayden, M. R. (2003) *Clin. Genet.* **64,** 210–215
8. Gros-Louis, F., Meijer, I. A., Hand, C. K., Dube, M. P., MacGregor, D. L., Seni, M. H., Devon, R. S., Hayden, M. R., Andermann, F., Andermann, E., and Rouleau, G. A. (2003) *Ann. Neurol.* **53,** 144–145
9. Ohtsubo, M., Kai, R., Furuno, N., Sekiguchi, T., Sekiguchi, M., Hayashida, H., Kuma, K., Miyata, T., Fukushige, S., Murotsu, T., Matsubara, K., and Nishimoto, T. (1987) *Genes Dev.* **1,** 585–593
10. Rosa, J. L., Casaroli-Marano, R. P., Buckler, A. J., Vilaro, S., and Barbacid, M. (1996) *EMBO J.* **15,** 4242–4273
11. Garcia-Gonzalo, F. R., Munoz, P., Gonzalez, E., Casaroli-Marano, R. P., Vilaro, S., Bartrons, R., Ventura, F., and Rosa, J. L. (2004) *FEBS Lett.* **559,** 77–83
12. Garcia-Gonzalo, F. R., Cruz, C., Munoz, P., Mazurek, S., Eigenbrodt, E., Ventura, F., Bartrons, R., and Rosa, J. L. (2003) *FEBS Lett.* **539,** 78–84
13. Roig, J., Mikhailov, A., Belham, C., and Avruch, J. (2002) *Genes Dev.* **16,** 1640–1658
14. Schimit, A., and Hall, A. (2002) *Genes Dev.* **16,** 1587–1609
15. Burd, C. G., Mustol, P. A., Schu, P. V., and Emr, S. D. (1996) *Mol. Cell. Biol.* **16,** 2369–2377
16. Horiuchi, H., Lippe, R., McBride, H. M., Rubino, M., Woodman, P., Stenmark, H., Rybin, V., Wilm, M., Ashman, K., Mann, M., and Zerial, M. (1997) *Cell* **90,** 1149–1159
17. Han, L., Wong, D., Dhaka, A., Afar, D., White, M., Xie, W., Herschman, H., Witte, O., and Colicelli, J. (1997) *Proc. Natl. Acad. Sci. U. S. A.* **94,** 4954–4959
18. Tall, G. G., Barbieri, M. A., Stahl, P. D., and Horazdovsky, B. F. (2001) *Dev. Cell* **1,** 73–82
19. Saito, K., Murai, J., Kajiho, H., Kontani, K., Kurosu, H., and Katada, T. (2002) *J. Biol. Chem.* **277,** 3412–3418
20. Kajiho, H., Saito, K., Tsujita, K., Kontani, K., Araki, Y., Kurosu, H., and Katada, T. (2003) *J. Cell Sci.* **116,** 4159–4168
21. Takeshima, H., Komazaki, S., Nishi, M., Iino, M., and Kangawa, K. (2000) *Mol. Cell* **6,** 11–22
22. Dasso, M. (2001) *Cell* **104,** 321–324
23. Etienne-Manneville, S., and Hall, A. (2002) *Nature* **420,** 629–635
24. Van Aelst, L., and Symons, M. (2002) *Genes Dev.* **16,** 1032–1054
25. Snider, W. D., Zhou, F. Q., Zhong, J., and Markus, A. (2002) *Neuron* **35,** 13–16
26. Luo, L. (2000) *Nat. Rev. Neurosci.* **1,** 173–180
27. Da Silva, J. S., and Dotti, C. G. (2002) *Nat. Rev. Neurosci.* **3,** 694–704
28. Zerial, M., and McBride, H. (2001) *Nat. Rev. Mol. Cell. Biol.* **2,** 107–117
29. Vetter, I. R., and Wittinghofer, A. (2001) *Science* **294,** 1299–1304
30. Otomo, A., Hadano, S., Okada, T., Mizumura, H., Kunita, R., Nishijima, H., Showguchi-Miyata, J., Yanagisawa, Y., Kohiki, E., Suga, E., Yasuda, M.,

Osuga, H., Nishimoto, T., Narumiya, S., and Ikeda, J.-E. (2003) *Hum. Mol. Genet.* **12,** 1671–1687
31. Topp, J. D., Gray, N. W., Gerard, R. D., and Horazdovsky, B. F. (2004) *J. Biol. Chem.* **279,** 24612–24623
32. Yamanaka, K., Vande Velde, C., Eymard-Pierre, E., Bertini, E., Boespflug-Tanguy, O., and Cleveland, D. W. (2003) *Proc. Natl. Acad. Sci. U. S. A.* **100,** 16041–16046
33. Stenmark, H., Vitale, G., Ullrich, O., and Zerial, M. (1995) *Cell* **83,** 423–432
34. Rybin, V., Ullrich, O., Rubino, M., Alexandrov, K., Simon, I., Seabra, M. C., Goody, R., and Zerial, M. (1996) *Nature* **383,** 266–269
35. Lippe, R., Miaczynska, M., Rybin, V., Runge, A., and Zerial, M. (2001) *Mol. Biol. Cell* **12,** 2219–2228
36. Koh, C. G., Manser, E., Zhao, Z. S., Ng, C. P., and Lim, L. (2001) *J. Cell Sci.* **114,** 4239–4251
37. Kim, S., Lee, S. H., and Park, D. (2001) *J. Biol. Chem.* **276,** 10581–10584
38. Zhu, K., Debreceni, B., Bi, F., and Zheng, Y. (2001) *Mol. Cell. Biol.* **21,** 425–437
39. Anborgh, P. H., Qian, X., Papageorge, A. G., Vass, W. C., DeClue, J. E., and Lowy, D. R. (1999) *Mol. Cell. Biol.* **19,** 4611–4622
40. Eisenhaure, T. M., Francis, S. A., Willison, L. D., Coughlin, S. R., and Lerner, D. J. (2003) *J. Biol. Chem.* **278,** 30975–30984
41. Chikumi, H., Barac, A., Behbahani, B., Gao, Y., Teramoto, H., Zheng, Y., and Gutkind, J. S. (2004) *Oncogene* **23,** 233–240
42. Kanekura, K., Hashimoto, Y., Niikura, T., Aiso, S., Matsuoka, M., and Nishimoto, I. (2004) *J. Biol. Chem.* **279,** 19247–19256

FEBS Letters 575 (2004) 64–70 FEBS 28783

# ALS2CL, the novel protein highly homologous to the carboxy-terminal half of ALS2, binds to Rab5 and modulates endosome dynamics ☆

Shinji Hadano[a,b], Asako Otomo[a], Kyoko Suzuki-Utsunomiya[a], Ryota Kunita[b], Yoshiko Yanagisawa[b], Junko Showguchi-Miyata[a], Hikaru Mizumura[b], Joh-E Ikeda[a,b,c,*]

[a]*Department of Molecular Neuroscience, The Institute of Medical Sciences, Tokai University, Isehara, Kanagawa 259-1193, Japan*
[b]*Solution Oriented Research for Science and Technology (SORST), Japan Science and Technology Agency, Tokai University School of Medicine, Isehara, Kanagawa 259-1193, Japan*
[c]*Department of Paediatrics, Faculty of Medicine, University of Ottawa, Ottawa, Ont., Canada K1H 8M5*

Received 10 May 2004; revised 5 July 2004; accepted 27 July 2004

Available online 7 September 2004

Edited by Lukas Huber

**Abstract ALS2, the causative gene product for juvenile recessive amyotrophic lateral sclerosis (ALS2), is a guanine-nucleotide exchange factor for the small GTPase Rab5. Here, we report a novel *ALS2* homologous gene, ALS2 C-terminal like (*ALS2CL*), which encodes a 108-kD ALS2CL protein. ALS2CL exhibited a specific but a relatively weak Rab5-GEF activity with accompanying rather strong Rab5-binding properties. In HeLa cells, co-expression of ALS2CL and Rab5A resulted in a unique tubulation phenotype of endosome compartments with significant colocalization of ALS2CL and Rab5A. These results suggest that ALS2CL is a novel factor modulating the Rab5-mediated endosome dynamics in the cells.**


*Keywords:* ALS2 carboxy-terminal like; Amyotrophic lateral sclerosis 2; Guanine-nucleotide exchange factor; Rab5; Endosome dynamics

## 1. Introduction

Amyotrophic lateral sclerosis (ALS), primary lateral sclerosis (PLS), and hereditary spastic paraplegia (HSP) are neurological disorders, which are characterized by a progressive motor neuronal degeneration [1,2]. Recently, we and other groups have identified the loss-of-functional mutations in the *ALS2* gene, accounting for a number of juvenile recessive motor neuron diseases (MND) including a type of juvenile ALS (ALS2), juvenile-onset PLS (PLSJ), and infantile-onset ascending hereditary spastic paralysis (IAHSP) [3–7].

The *ALS2* gene encodes a novel 184 kD protein, termed ALS2 or alsin, comprising three predicted guanine-nucleotide exchange factor (GEF) domains [3,4]; i.e., regulator of chromosome condensation (RCC1) [8]-like domain (RLD), the Dbl homology and pleckstrin homology (DH/PH) domains [9], and a vacuolar protein sorting 9 (VPS9) domain [10,11]. In addition, eight consecutive membrane occupation and recognition nexus (MORN) motifs [12] are noted in the region between DH/PH and VPS9 domains [13]. Recently, we have identified the ALS2-associated Rab5-specific GEF activity that is mediated by the carboxy-terminal MORN/VPS9 domain of ALS2 and also shown that ALS2 localizes preferentially onto the early endosome compartments in neuronal cells [13]. Since Rab5 plays crucial roles in clathrin-mediated vesicle endocytosis, trafficking, and early endosomal membrane fusion [14], ALS2 may implicate in the vesicle/membrane dynamics in the cells through the activation of Rab5.

Here, we report the identification and characterization of the novel *ALS2* homologous gene, ALS2 C-terminal like (*ALS2CL*/*Als2cl*), and its gene product ALS2CL.

## 2. Materials and methods

### 2.1. Cloning of the ALS2 homologous genes

To identify the potential homologs/paralogs for *ALS2*/*Als2* genes, we conducted BLAST searches [15] on the public databases. Cloning of the full-length transcripts for the identified homologous genes, i.e., *ALS2CL* and *Als2cl*, was performed by a reverse transcriptase (RT)-polymerase chain reaction (PCR)-based method. Analysis of the predicted amino acid sequences, including motif/domain identification and multiple protein sequence alignment was conducted as described [3].

### 2.2. Northern blotting

Multiple human adult tissue Northern (MTN) blot (Clontech) was hybridized with [α-$^{32}$P]dCTP-labeled open reading frame (ORF) probes generated from the *ALS2CL* or *ACTB* (β-actin) cDNA in PerfectHyb hybridization solution (Toyobo) at 68 °C. Membranes were washed with 0.1× SSC containing 1% SDS at 65 °C and exposed to X-ray film (Bio-MAX, Kodak). The mouse adult tissue MTN blot (Clontech) was also hybridized with the *Als2cl* or glyceraldehyde 3-phosphate dehydrogenase (*Gapdh*) cDNA.

☆ The cDNA sequences of *ALS2CL* and *Als2cl* have been deposited in DDBJ/EMBL/GenBank Database under Accession Nos. AB107015 and AB107016.

* Correspondence author. Fax: +81-463-91-4993.
*E-mail address:* joh-e@nga.med.u-tokai.ac.jp (J.-E. Ikeda).

*Abbreviations:* ALS, amyotrophic lateral sclerosis; PLS, primary lateral sclerosis; HSP, hereditary spastic paraplegia; MND, motor neuron disease; ALS2CL, ALS2 carboxy-terminal like; GEF, guanine-nucleotide exchange factor; RLD, regulator of chromosome condensation-like domain; DH, Dbl homology; PH, pleckstrin homology; MORN, membrane occupation and recognition nexus; VPS9, vacuolar protein sorting 9; EEA1, early endosome antigen-1; EGFP, enhanced green fluorescent protein

0014-5793/$22.00 
doi:10.1016/j.febslet.2004.07.092

*2.3. Expression constructs*

All cDNA expression constructs were generated by subcloning the RT-PCR amplified fragments into the appropriate vectors. For the GEF assay, four cDNA fragments; i.e., human ALS2_1018-1657aa (ALS2_1018-1657), human *ALS2CL* ORF (ALS2CL_human), and mouse *Als2cl* ORF (ALS2CL_mouse), were subcloned into pCI-neo Mammalian Expression Vector (Promega). For the subcellular localization studies, human and mouse ALS2CLs, which were fused amino-terminally with enhanced green fluorescent protein (EGFP), were generated using pEGFP-C1 (Clontech). The bacterial expression plasmids encoding the small GTPases and FLAG-tagged human Rab5A, which have been previously generated [13], were also utilized.

*2.4. GEF assay and in vitro binding*

GEF assay was conducted as previously described [13]. In vitro binding experiments were also performed as described [13] with several modifications. In brief, purified Rab5A (4 pmol), which was pre-loaded with either GDP or GTPγS, or nucleotide-free, was mixed with FLAG-M2 beads conjugating 4 pmol equivalent of the immunoprecipitated FLAG-tagged ALS2CL or ALS2 in 100 μl of a modified GEF buffer [25 mM Tris–HCl, pH 7.4, 100 mM NaCl, 20 mM $MgCl_2$, 1.5 mM CHAPS, and 0.1% (w/v) skimmed milk] containing 50 μM of either GDP or GTPγS, or without nucleotides, for 2 h at 30 °C. After washing with 4 × 1 ml of the same buffer, bound Rab5A was co-eluted with FLAG-ALS2CL protein by the addition of SDS–PAGE sample buffer and detected by Western blotting analysis using appropriate antibodies.

*2.5. Cell culture, transfection, and microscopic observations*

HeLa and COS-7 cells were cultured in Dulbecco's modified Eagle's medium supplemented with 10% fetal bovine serum (Invitrogen), 100 U/ml penicillin, and 100 μg/ml streptomycin. Cells were transfected with plasmid constructs using Effectene Transfection Reagent (Qiagen). Immunocytochemical detection and image analysis were conducted by Leica TCS_NT confocal-microscope systems (Leica) as previously described [13].

## 3. Results

*3.1. Identification of the human ALS2CL and mouse Als2cl genes*

A BLAST search of the GenBank/DDBJ/EMBL database for potential *ALS2/Als2* paralogs and/or homologs revealed the presence of the genomic segments, mRNAs, and EST sequences, which encode a novel protein highly homologous to the carboxy-terminal half of the human and mouse ALS2 proteins, in human, mouse, and rat genome. Computational analyses of the DNA sequences by assembling the mRNA and EST sequences, followed by the comparison with genomic DNA sequences and mapping, demonstrated that human and mouse *ALS2/Als2* homologous genes comprised 26 exons and resided within approximately 24.5 kb of the genomic region on human chromosome 3p21.31 and the 23.2 kb genomic region on mouse chromosome 9F3, respectively (Fig. 1A). We designated these human and mouse genes as ALS2 C-terminal like; *ALS2CL* (HGNC approved symbol) and *Als2cl* (MGD nomenclature committee approved symbol), respectively. The sequences of the *ALS2CL* and *Als2cl* transcripts encompassed 4741 nt (ORF; 2862-nt long) (AB107015) and 5081 nt (ORF; 2859-nt long) (AB107016), and matched with the sequences for human transcript LOC259173_isoform 1 (NM_147129) and mouse RN49018 (NM_146228) [16], respectively (Fig. 1A and B).

*3.2. Alternative splicing variants for ALS2CL and Als2cl*

In the course of our database searches and RT-PCR based cloning of the transcribed DNA sequences, an extensive alternative splicing of the transcripts, giving rise to at least 17 minor variants of *ALS2CL*, was noted in human tissues (Fig. 1B), in addition to the major *ALS2CL* transcript. Analyses of the flanking DNA sequences for these variants identified the cryptic acceptor and donor consensus sequences (data not shown), suggesting that all these variants arose by alternative splicing. It was also evident that all these alternative splicing, resulting in premature stop codons, disrupted the coding frame for full-length *ALS2CL* (Fig. 1B). Physiological significances of these extensive splicing events were currently unknown.

We also identified five minor murine variants as follows: (1) alternative 5′-UTR exons **'a'** and **'b'** proceeded by exon 2 (Fig. 1A), (2) cryptic three nucleotides insertion (-27_-26insTAG), (3) transcript with intron 13, (4) transcripts with skipping exon 19, and (5) alternative exon **'c'** between exons 7 and 8 (RIKEN_5830412B02: with skipping exon 19, Fig. 1A).

*3.3. Deduced amino acid sequences*

Computational predictions have shown that major transcripts for both *ALS2CL* and *Als2cl* encode 108-kD proteins, ALS2CL [953 and 952 amino acids (aa), respectively], comprising several domains and motifs including PH, MORN, and VPS9 (Fig. 2A). Human and mouse ALS2CL proteins showed a high degree of sequence conservation to each other (81% identity and 88% similarity), and with the corresponding C-terminal region of human ALS2 (33% identity and 51% similarity) (Fig. 2B). Interestingly, phylogenetical analysis revealed that amino acid sequences for ALS2CL were much closer to that for fugu ALS2 than those for human and mouse ALS2 (data not shown).

*3.4. Tissue distribution of the ALS2CL/Als2cl mRNA*

Northern blot analysis revealed the *ALS2CL* transcript of an approximately 5 kb of the major mRNA in various adult human tissues with higher expression in both heart and kidney (Fig. 3A). It is also noted that the band-signals for the *ALS2CL* transcript were rather blurred, consistent with the presence of multiple alternative splicing variants. In contrast, a single 5 kb discrete band for the mouse *Als2cl* transcript was observed in variety of tissues in adult mice with highest in liver (Fig. 3B).

*3.5. Assays of the ALS2CL-associated GEF activity*

To analyze the ALS2CL-associated GDP/GTP exchanging activities, i.e., so-called GEF activities, on the small GTPases, in vitro GDP dissociation assays were conducted using nine bacterially produced small GTPases including Rab4A, Rab5A, Rab5B, Rab5C, Rab7, Rab11A, Rac1, RhoA, and Cdc42. The ALS2_1018-1657 peptide, which spans the minimum region associating with Rab5-GEF activity [13], was used as a positive control. The results showed that human ALS2CL exclusively catalyzed GDP dissociation on Rab5A, Rab5B, and Rab5C, as in the cases for ALS2_1018-1657 (Fig. 4A), suggesting that humanALS2CL retained selective catalytic activity with all the members of Rab5 family. However, the degree of activities for ALS2CL was significantly lower than that for ALS2_1018-1657 (Fig. 4A). Interestingly, mouse ALS2CL exhibited almost no Rab5-GEF activities (Fig. 4A).

To define the enzymatic kinetics for the Rab5GEF activity, we next carried out the GDP dissociation assay on Rab5A using a wide range of concentrations for either ALS2CLs or

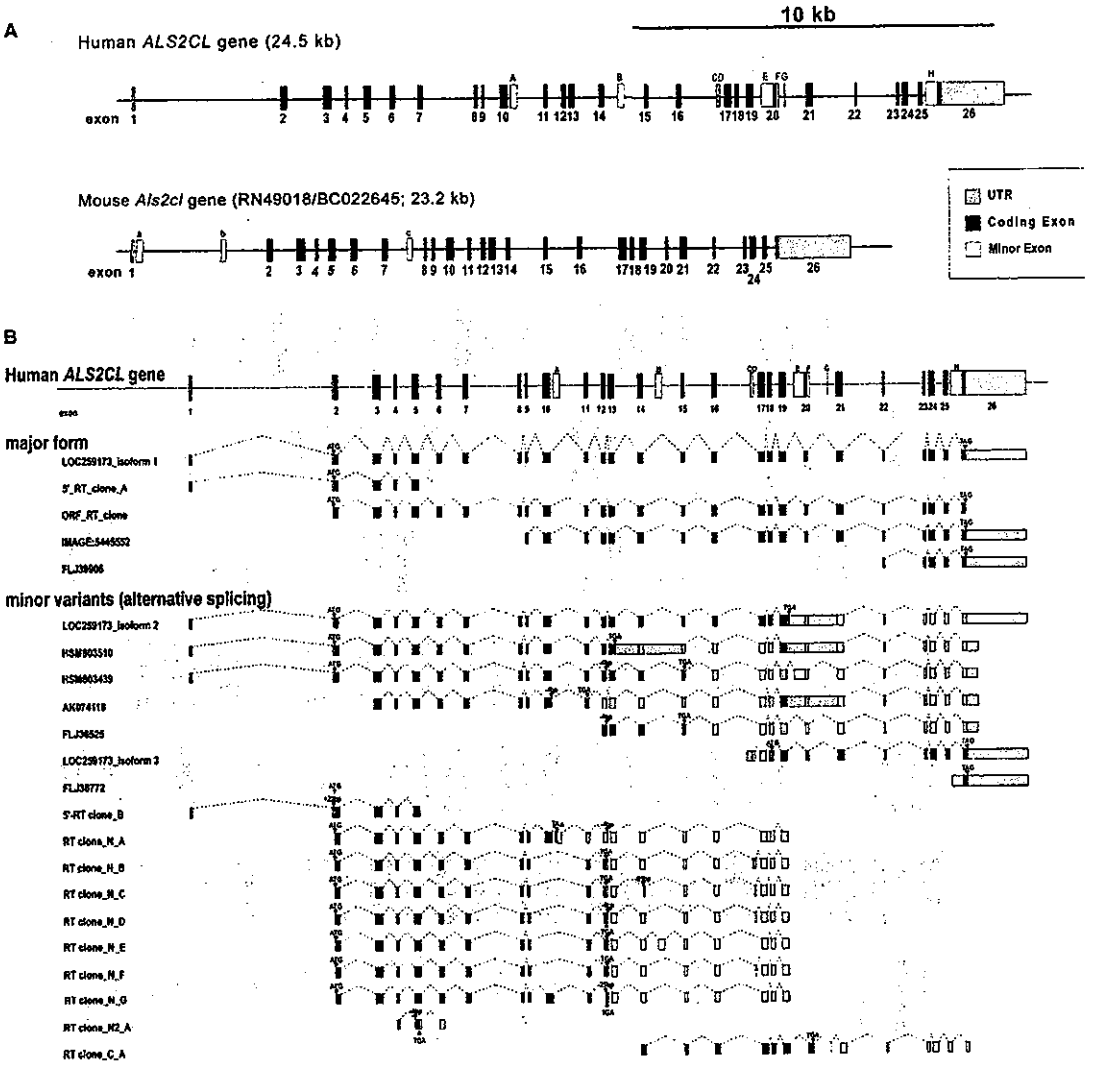


Fig. 1. Genomic organization of the human *ALS2CL* and mouse *Als2cl* genes. (A) Schematic representation of genomic organizations for human *ALS2CL* (upper) and mouse *Als2cl* (lower) genes. *ALS2CL* spans approximately 24.5 kb of the genomic region on human chromosome 3p21.31, while *Als2cl* covers approximately 23.2 kb of the region on chromosome 9F3. Both genes comprise 26 major exons. Black and gray boxes represent coding (translated) and non-coding (untranslated) region of major exons (exons 1–26), respectively. Minor alternative exons (A–H for human; a–c for mouse) are also shown as white boxes. (B) Exon organization of splicing variants for the human *ALS2CL* transcripts. A single major form and 17 differentially spliced minor variants are shown. The positions of translation initiation (ATG) and termination (TGA, TAG, or TAA) codons are shown.

ALS2_1018-1657 (final 0–1.6 μM) (Fig. 4B). Both ALS2_1018-1657 and human ALS2CL revealed the protein concentration-dependent Rab5-GEF activities with approximately eightfold lower dissociation constant with human ALS2CL (ALS2_1018-1657; ~25 nM vs. human ALS2CL; ~200 nM). However, mouse ALS2CL did not show any significant Rab5-GEF activities at any concentrations of the protein (Fig. 4B).

### 3.6. Interaction of ALS2CL and Rab5

To examine whether the ALS2CL proteins directly interact with Rab5, we conducted the in vitro binding assays using the FLAG-M2 pull-down experiments. The amino-terminally FLAG-tagged ALS2_1018-1657, human ALS2CL, and mouse ALS2CL were immunoprecipitated in the presence of recombinant Rab5A, which was pre-loaded with either GDP or GTPγS, or left unloaded with any nucleotides. Despite the fact that the ALS2CL proteins showed a low or negligible Rab5-GEF activity, they bound rather strongly to Rab5A (Fig. 5). Notably, the ALS2_1018-1657 peptide, which revealed the higher Rab5-GEF activity (Fig. 4), bound preferentially to the nucleotide-free form of Rab5A, whereas mouse ALS2CL, which exhibited no Rab5-GEF activity, interacted non-selectively with any forms of Rab5A. The Rab5A-binding properties for human ALS2CL demonstrated an intermediate preferentiality.

### 3.7. Subcellular localization of ALS2CL

To investigate the subcellular localization of ALS2CL, HeLa cells were transfected with plasmid expressing either human or mouse ALS2CL. Ectopically expressed amino-terminally

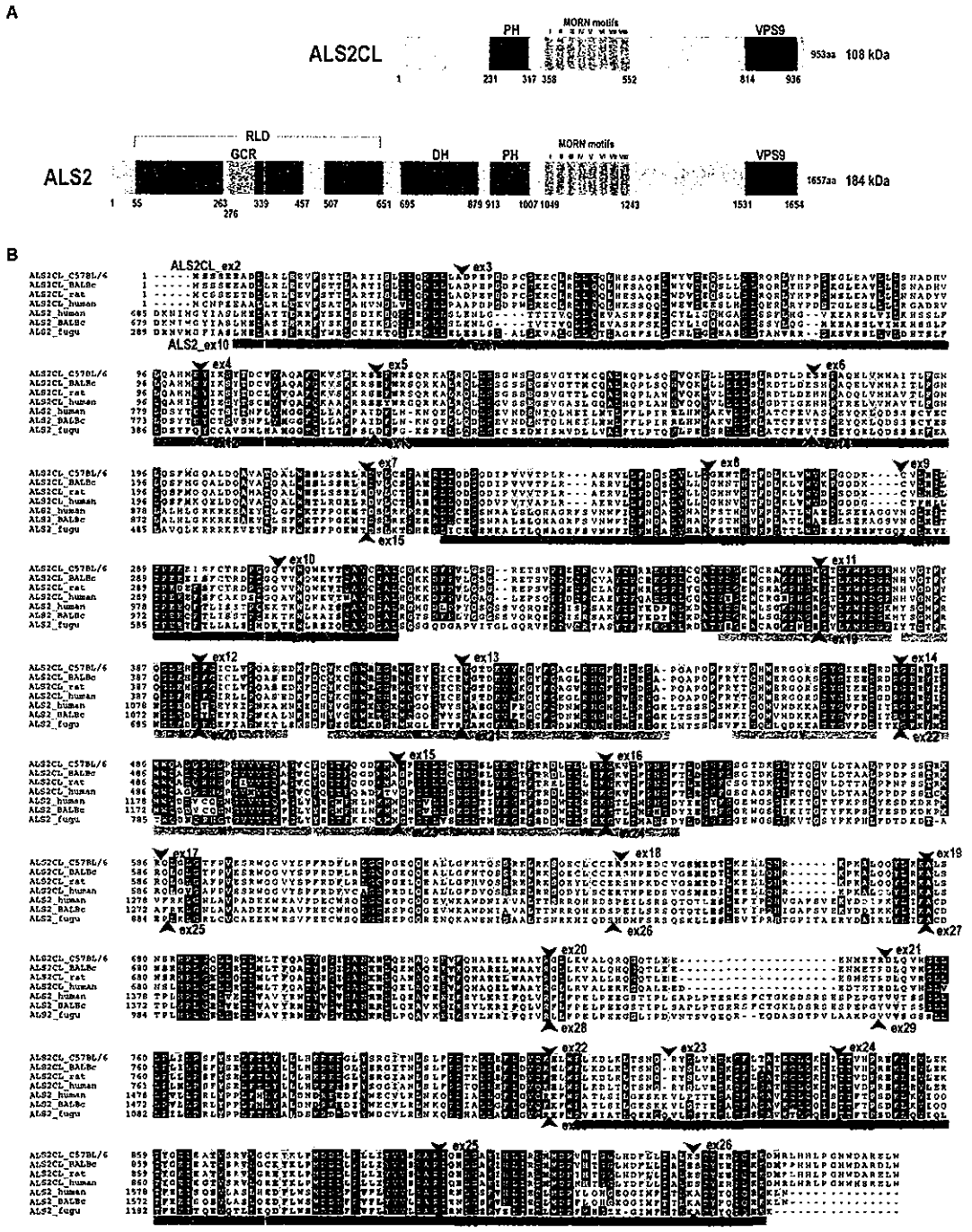


Fig. 2. Amino acid sequence analysis. (A) Schematic representation of the domains and motifs identified in the predicted human ALS2CL and ALS2 proteins. (B) ClustalW multiple amino acid sequence alignment of mouse (ALS2CL_C57BL/6; NP_666340, and ALS2CL_BALBc; this study), rat (ALS2CL_rat; XP_236654), and human (ALS2CL_human; this study) ALS2CL proteins, and the C-terminal portions of human (ALS2_human; NP_065970), mouse (ALS2_BALBc; NP_082993), and fugu (ALS2_fugu; SINFRUP00000067515) ALS2 proteins. Intron–exon boundaries for human *ALS2CL* and *ALS2* are also shown. Sequences are numbered with the initiation codon of each protein as #1.

FLAG-tagged (Fig. 6A) and EGFP-fused (Fig. 6B) human ALS2CL proteins localized throughout the cells with strong punctated stainings in cytoplasm. EGFP-fused mouse ALS2CL also showed similar distribution pattern (Fig. 6C). Co-localization analyses revealed that human ALS2CL partially overlapped with early endosome antigen 1 (EEA1) [17] immunopositive vesicles and/or early endosomes (Fig. 6D–F), but not with the late-endosomal/lysosomal markers, LAMP-1

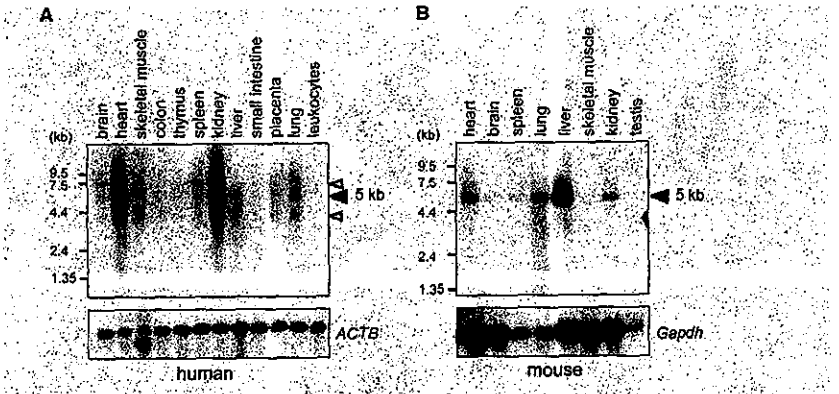


Fig. 3. Northern blot analysis. MTN blots were hybridized with *ALS2CL/Als2cl* (upper panel) cDNA clones. Filled and open arrowheads indicate the position of major and minor transcripts, respectively. The lower panel represents the same blots hybridized with (A) the human *ACTB* (β-actin) cDNA or (B) the mouse glyceraldehyde 3-phosphate dehydrogenase (*Gapdh*) cDNA to confirm RNA quality and relative loading. Positions of size-markers are shown on the left.

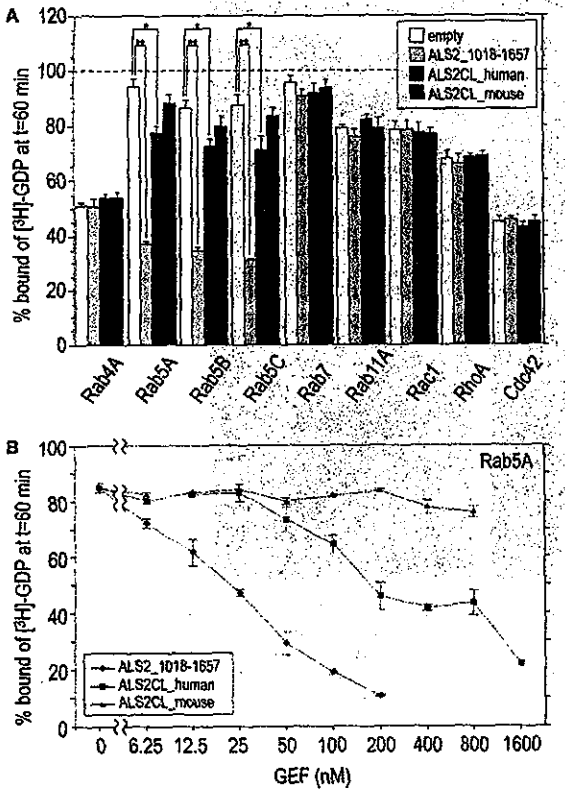


Fig. 4. GEF activity assays. (A) In vitro [$^3$H]GDP dissociation assay for FLAG-tagged ALS2 peptide (ALS2_1018-1657aa; light gray bars), human ALS2CL (ALS2CL_human; dark gray bars), mouse ALS2CL (ALS2CL_mouse; black bars), and FLAG-tag alone (empty; as a control, open bars) on nine different small GTPases. Each value represents the mean and standard deviation of at least three independent assays. Double asterisk, $P<0.001$; asterisk, $P<0.01$ in $t$ tests. (B) In vitro [$^3$H]GDP dissociation assay on Rab5A in the presence of increasing amount of recombinant ALS2CL and ALS2 proteins. Each value represents means ± S.D. ($n=3$) of the percentage of [$^3$H]-GDP bound to Rab5A after 60 min in the presence of given amount either of ALS2_1018-1657 (diamonds), ALS2CL_human (squares), or ALS2CL_mouse (triangles).

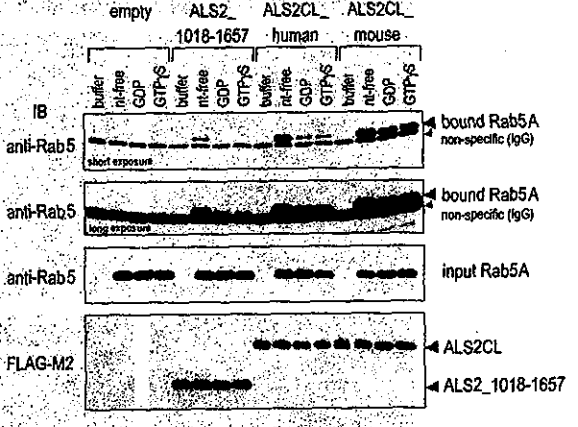


Fig. 5. In vitro Rab5A binding assay. Nucleotide free (nt-free), GDP bound (GDP), or GTPγS bound (GTPγS) forms of Rab5A were incubated with FLAG-M2 beads conjugating FLAG-tagged ALS2_1018-1657aa, human ALS2CL (ALS2CL_human), or mouse ALS2CL (ALS2CL_mouse), or with FLAG-M2 beads alone (empty) as a control. The bound and input Rab5A were detected by immunoblotting method using anti-Rab5 antibody. Western blotting analysis of the FLAG-tagged proteins was also conducted using the FLAG-M2 antibody.

and LAMP-2 [18], or Golgi marker GM130 [19] (data not shown). However, the degree of EEA1 overlapping was quite low (<10%), when compared with those for ALS2_660-1657, in which a high degree (~85%) of vesicular co-localization was observed [13].

### 3.8. Co-localization of ALS2CL and Rab5A

To investigate whether human ALS2CL co-localized with Rab5 in vivo, co-transfection of HeLa cells with expression constructs for EGFP-fused ALS2CL and FLAG-tagged Rab5A was conducted. The results showed that both proteins were significantly co-distributed onto the vesicular/membranous compartments in cytoplasm, particularly to the leading edges of the cells (Fig. 6G–I). Notably, co-expression of ALS2CL and Rab5A frequently (~40% of the co-transfected

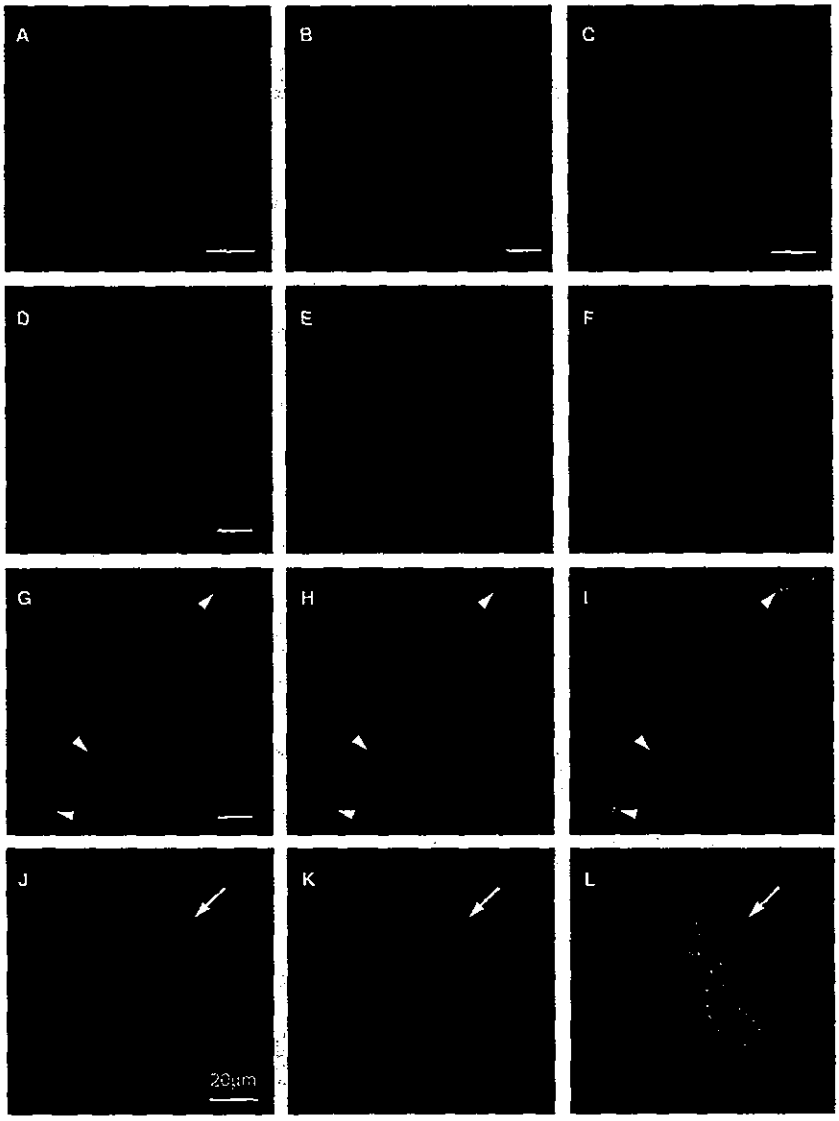


Fig. 6. Localization of ALS2CL in the cells. (A–C) Subcellular distribution of the ectopically expressed ALS2CL in HeLa cells (A, FLAG-tagged human ALS2CL; B, EGFP-fused human ALS2CL; C, EGFP-fused mouse ALS2CL). (D–F) Partial co-localization of the human ALS2CL onto EEA1-positive endosomes (D, EGFP-fused human ALS2CL; E, endogenous EEA1; F, merged image). (G–L) Co-transfection of the EGFP-fused human ALS2CL and FLAG-tagged Rab5A expression constructs in HeLa cells (G and J, EGFP-fused human ALS2CL; H and K, FLAG-tagged Rab5A; I and L, merged images). The representative images for the cells exhibiting vesicular (G–I) and tubular membranous (arrows; J–L) distributions are shown. Arrowheads indicate the leading edges of the cells.

cells) caused a striking effect on the morphology of endosomal compartments, showing a tubulation and/or elongation with accompanying extensive co-localization of ALS2CL and Rab5A (Fig. 6J–L).

## 4. Discussion

In this study, we newly identified the *ALS2* homologous gene, *ALS2CL* and *Als2cl*. *ALS2CL* and *Als2cl* map to the syntenic chromosomal regions on human chromosome 3p21 and mouse chromosome 9F3, respectively, both comprising 26 major exons. The intron–exon boundaries for *ALS2CL* and *Als2cl*, and those for the homologous regions of *ALS2*/*Als2* were nearly completely preserved. Further, analysis of the predicted amino acid sequences revealed a high level of sequence similarity throughout the entire region of ALS2CL and the C-terminal portion of the ALS2 proteins, indicating that *ALS2CL*/*Als2cl* and *ALS2*/*Als2* were evolutionally conserved genes evolved from a common ancestry of origin. Notably, *ALS2CL*/*Als2cl* lack several exons corresponding to those encoding N-terminal RLD for ALS2, suggesting that the N-

terminal portion of ALS2 can be independently evolved. In spite of such structural conservation, our results demonstrate that the molecular functions for ALS2CL and the C-terminal homologous region of ALS2 seem to be slightly different.

Previously, we have shown that enzymatic activity for the activation of Rab5 GTPase is retained in the C-terminal portion of human ALS2 comprising MORN/VPS9 domain, and that either deletion of MORN motifs or the mutation in the evolutionally conserved amino acid residues in VPS9 domain resulted in the loss of its catalytic activity [13]. In this study, we demonstrated that, although human ALS2CL showed a similar catalytic specificity on the small GTPases as that for human ALS2, the level of its Rab5-GEF activity was significantly lower than that for ALS2, or even at almost negligible levels. On the other hand, ALS2CL, especially an enzymatically almost-inactive mouse ALS2CL, exhibited a stronger binding to Rab5 than ALS2, in a nucleotide state-independent manner. These results suggest that ALS2CL may act as a functional modulator in the Rab5-mediated enzymatic reactions, whilst those actions are slightly different from that for ALS2.

We have previously also shown that overexpression of the C-terminal human ALS2 peptide containing 660–1657 aa, spanning a homologous region corresponding to entire ALS2CL, localizes onto the Rab5/EEA1-positive early endosomal compartments, and induces the striking enlargement of endosomes, which is mediated through the Rab5GEF activity inherent to the MORN/VPS9 region of ALS2 [13]. On the other hand, ectopically expressed ALS2CLs localize in both nucleus and cytoplasm with strong punctated stainings that are extensively overlapped with Rab5A but not with EEA1, suggesting that the ALS2CL proteins preferentially localize to the Rab5-positive/EEA1-negative vesicles and/or endosome sub-compartments. Further, co-expression of human ALS2CL and Rab5A caused unique morphological changes in endosomal compartments, which were characterized by membrane tubulation rather than enlargement. Taken together, these results again support the biochemical notion that ALS2CL and ALS2 mediate similar but slightly different molecular functions in the cells.

Several recent studies demonstrated that the similar tubular endosome phenotypes were elicited under certain experimental conditions, such as in the presence of wortmannin, an inhibitor for phosphatidylinositol-3 kinase [20], or brefeldin A, a potent inhibitor of trafficking through the secretory pathway [21], as well as by the overexpression of dominant positive Rab4 small GTPase [22]. As each of these treatments leads to the impairment of normal endosomal membrane trafficking [20–22], overexpression of human ALS2CL may also disturb the normal vesicle/membrane trafficking possibly through the actions associating with a lower Rab5-GEF activity with a higher Rab5 binding property for the ALS2CL proteins.

In summary, our results demonstrate that *ALS2CL/Als2cl* and *ALS2/Als2* are evolutionally conserved genes, and that their products, ALS2CL and ALS2, play overlapping but slightly distinctive roles on the Rab5-mediated vesicle/membrane trafficking and dynamics in the cells. Thus, it is possible that ALS2CL modulates the ALS2-mediated molecular and cellular functions either directly or indirectly, thereby implicating in the phenotypic variations seen in patients with ALS2/PLSJ/IAHSP. Further dissection of molecular and cellular functions for ALS2CL as well as those for ALS2 will give us additional insights into the pathogenesis for a number of MNDs caused by the *ALS2* mutations.

*Acknowledgements:* We thank all the members of our laboratory for helpful discussion. This work was funded by a Grant-in-Aid for Scientific Research from Japan Society for the Promotion of Science, the Sumitomo Foundation, the Naito Foundation, and the Japan Science and Technology Agency.

## References

[1] Cleveland, D.W. and Rothstein, J.D. (2001) Nat. Rev. Neurosci. 2, 806–819.
[2] Fink, J.K. (2001) Semin. Neurol. 21, 199–207.
[3] Hadano, S., Hand, C.K., Osuga, H., Yanagisawa, Y., Otomo, A., Devon, R.S., Miyamoto, N., Showguchi-Miyata, J., Okada, Y., Singaraja, R., Figlewicz, D.A., Kwiatkowski, T., Hosler, B.A., Sagie, T., Skaug, J., Nasir, J., Brown Jr., R.H., Scherer, S.W., Rouleau, G.A., Hayden, M.R. and Ikeda, J.-E. (2001) Nat. Genet. 29, 166–173.
[4] Yang, Y., Hentati, A., Deng, H.X., Dabbagh, O., Sasaki, T., Hirano, M., Hung, W.Y., Ouahchi, K., Yan, J., Azim, A.C., Cole, N., Gascon, G., Yagmour, A., Ben-Hamida, M., Pericak-Vance, M., Hentati, F. and Siddique, T. (2001) Nat. Genet. 29, 160–165.
[5] Eymard-Pierre, E., Lesca, G., Dollet, S., Santorelli, F.M., di Capua, M., Bertini, E. and Boespflug-Tanguy, O. (2002) Am. J. Hum. Genet. 71, 518–527.
[6] Gros-Louis, F., Meijer, I.A., Hand, C.K., Dube, M.P., MacGregor, D.L., Seni, M.H., Devon, R.S., Hayden, M.R., Andermann, F., Andermann, E. and Rouleau, G.A. (2003) Ann. Neurol. 53, 144–145.
[7] Devon, R.S., Helm, J.R., Rouleau, G.A., Leitner, Y., Lerman-Sagie, T., Lev, D. and Hayden, M.R. (2003) Clin. Genet. 64, 210–215.
[8] Ohtsubo, M., Kai, R., Furuno, N., Sekiguchi, T., Sekiguchi, M., Hayashida, H., Kuma, K., Miyata, T., Fukushige, S. and Murotsu, T. (1987) Genes. Dev. 1, 85–593.
[9] Schmidt, A. and Hall, A. (2002) Genes Dev. 16, 1587–1609.
[10] Burd, C.G., Mustol, P.A., Schu, P.V. and Emr, S.D. (1996) Mol. Cell. Biol. 16, 2369–2377.
[11] Horiuchi, H., Lippe, R., McBride, H.M., Rubino, M., Woodman, P., Stenmark, H., Rybin, V., Wilm, M., Ashman, K., Mann, M. and Zerial, M. (1997) Cell 90, 1149–1159.
[12] Takeshima, H., Komazaki, S., Nishi, M., Iino, M. and Kangawa, K. (2000) Mol. Cell 6, 11–22.
[13] Otomo, A., Hadano, S., Okada, T., Mizumura, H., Kunita, R., Nishijima, H., Showguchi-Miyata, J., Yanagisawa, Y., Kohiki, E., Suga, E., Yasuda, M., Osuga, H., Nishimoto, T., Narumiya, S. and Ikeda, J.-E. (2003) Hum. Mol. Genet. 12, 1671–1687.
[14] Zerial, M. and McBride, H. (2001) Nat. Rev. Mol. Cell Biol. 2, 107–117.
[15] Altschul, S.F., Madden, T.L., Schaffer, A.A., Zhang, J., Zhang, Z., Miller, W. and Lipman, D.J. (1997) Nucl. Acids Res. 25, 3389–3402.
[16] Mitchem, K.L., Hibbard, E., Beyer, L.A., Bosom, K., Dootz, G.A., Dolan, D.F., Johnson, K.R., Raphael, Y. and Kohrman, D.C. (2002) Hum. Mol. Genet. 11, 1887–1898.
[17] Mu, F.T., Callaghan, J.M., Steele-Mortimer, O., Stenmark, H., Parton, R.G., Campbell, P.L., McCluskey, J., Yeo, J.P., Tock, E.P. and Toh, B.H. (1995) J. Biol. Chem. 270, 13503–13511.
[18] Fukuda, M. (1994) Subcell. Biochem. 22, 199–230.
[19] Barr, F.A., Nakamura, N. and Warren, G. (1998) EMBO J. 17, 3258–3268.
[20] Shpetner, H., Joly, M., Hartley, D. and Cotvera, S. (1996) J. Cell Biol. 132, 595–605.
[21] de Figueiredo, P., Doody, A., Polizotto, R.S., Drecktrah, D., Wood, S., Banta, M., Strang, M.S. and Brown, W.J. (2001) J. Biol. Chem. 276, 47361–47370.
[22] McCaffrey, M.W., Bielli, A., Cantalupo, G., Mora, S., Roberti, V., Santillo, M., Drummond, F. and Bucci, C. (2001) FEBS Lett. 495, 21–30.

<シンポジウム3—4>脊髄小脳変性症と運動ニューロン疾患

# 劣性遺伝の運動ニューロン疾患：ALS2遺伝子変異と神経細胞死の機序

池田　穣衛

臨床神経学　第44巻　第11号　別刷
（2004年11月1日発行）

<シンポジウム3―4>脊髄小脳変性症と運動ニューロン疾患

# 劣性遺伝の運動ニューロン疾患：ALS2遺伝子変異と神経細胞死の機序

池田　穣衛

（臨床神経，44：792―794，2004）
Key words：家族性筋萎縮性側索硬化症，ALS2遺伝子，グアニンヌクレオチド交換因子，エンドソーム情報伝達

## はじめに

若年性筋萎縮性側索硬化症2型（ALS2）は常染色体劣性遺伝形式を示す上位運動ニューロン変性疾患である．ALS2の遺伝子座はヒト第2染色体長腕q33領域にマップされている．私達はこの領域から新規遺伝子ALS2(全長約80kbp，34個のエクソンをコードしている)を単離し，当該遺伝子のエクソン中にALS2患者に特異的な欠失変異（homozygous deletion mutation)をみいだした．これらの欠失変異はALS2遺伝子産物（ALS2蛋白質，推定1657アミノ酸残基，184kDa）の蛋白質コードフレームを壊し不完全長ALS2蛋白質の産生によるALS2機能喪失変異であることが明らかになった．これらのことから，私達はALS2遺伝子変異がALS2発症の主因であると同定した．その後，上位運動ニューロンの変性を病徴とするjuvenile primary lateral sclerosisやinfantile-ascending hereditary spastic paralysisにおいてもALS2遺伝子変異が同定され，今日までに独立した9家系においてそれぞれことなる9個のhomozygous ALS2 mutationが同定されている．このことから，上位運動神経変性の主因はALS2蛋白質の機能欠損であると考えられる．続いて，私達はALS2蛋白質が低分子G蛋白質Rab5を基質とするグアニンヌクレオチド交換因子（GEF）活性を有する事，ALS2蛋白質はこの活性を背景とする神経細胞シグナル伝達にかかわるエンドソーム分子動態にかかわる事を確認した．さらに，私達はALS2モデル動物としてALS2 KO mouseを作出しており，本稿ではALS2遺伝子機能と併せて上位運動神経変性の分子機序について考察する．

## ALS2の臨床的特徴

ALS2は上位運動ニューロンの変性にともなう四肢，顔面，咽頭筋の痙攣，構音障害などの偽球麻痺症状，および進行性の四肢筋萎縮等の諸症状を特徴とする．発症年齢は平均6.9歳と若年発症型である一方，病状の進行はきわめて緩徐である．本疾患の初期症状は若年発症型の原発性側索硬化症（juvenile primary lateral sclerosis；JPLS）と酷似している[1]．

## ALS2遺伝子と機能

筋萎縮性側索硬化症（amyotrophic lateral sclerosis；ALS）は大脳皮質錐体細胞から脊髄にいたる上位運動ニューロンおよび脊髄前角細胞から筋にいたる下位運動ニューロンが選択的に障害される進行性神経変性疾患である．ALS発症の分子機序は未だ明らかでなく，治療法も確立されていないのが現状である．ALS患者の大多数は孤発例であるが，5～10%の患者は家族性（遺伝性）ALSと考えられている．家族性ALS（FALS）については，優性遺伝形式をとるALS1，ALS3，ALS4，ALS6およびFTD-ALS，そして劣性遺伝形式をとるALS2，ALS5，およびType 2とX染色体連鎖を示すALSXがそれぞれ報告されている．ヒトゲノム解析を背景に，今日までに漸く2つのALS発症責任遺伝子の同定に成功している．最初に，Rosenら[2]は優性遺伝形式をとるALS1の責任遺伝子としてCu-Zn superoxide dismutase 1（SOD1）遺伝子を同定した．当初はSOD1変異による神経細胞内でのフリーラジカルの集積が運動神経変性をもたらす要因となっていると推定したが，その後の一連の解析によってALS1にみられる神経細胞死はむしろ変異SOD1タンパク質の異型機能（toxic gain-of-function）による奇形複合体形成によるのではないかと推測されるにいたっているがその本態はまだ不明である．

SOD1遺伝子に次ぐ2つ目のALS発症責任遺伝子として，私達は劣性遺伝形式をとる若年性筋萎縮性側索硬化症2型（ALS2）の発症責任遺伝子；ALS2遺伝子の同定に成功した[3][4]．ALS2患者にみいだされたALS2遺伝子変異はすべて当該遺伝子のエクソン中の1および2bpの欠失変異（homozygous deletion mutation）であることから，これらの欠失変異はALS2遺伝子産物（ALS2蛋白質，推定1657アミノ酸残基，184kDa）の蛋白質コードフレームを壊し不完全長ALS2蛋白質を作ると考えられる．したがって，ALS2にみられる運動ニューロンの変性はALS2機能喪失（loss-of-function）によると考えられる．その後，juvenile primary lateral sclerosis（JPLS）やinfantile-ascending hereditary spas-

東海大学大学院医学研究科　脳・神経疾患研究センター〔〒259-1193　神奈川県伊勢原市望星台〕
（受付日：2004年5月12日）

tic paralysis (IAHSP) においてもALS2遺伝子変異が同定された．今日までに独立した9家系においてそれぞれことなる9個のhomozygous ALS2 mutation（1bpあるいは2，10bpのhomozygous deletionによるフレームシフト変異およびナンセンス変異）[3)-7)]が同定されている．これらすべての患者例において，不完全長ALS2蛋白質が産生され，ALS2正常機能が損なわれていると思われる．ALSでは上位と下位の運動ニューロンが障害されるのに対して，PLSやHSPでの神経変性は上位運動ニューロンに限定されている．したがって，ALS2蛋白質の機能喪失が上位運動神経変性を特徴とするALS2やJPLS，IAHSP発症の原因であることから，ALS2蛋白質は上位運動神経の機能と生存に必須であるといえる．ALS2蛋白質の機能としては，3種類の低分子G蛋白質の機能調節因子グアニンヌクレオチド交換因子（RanGEF，RhoGEF，Rab5GEF）機能ドメインの他に膜結合ドメインなどが推定されている．

私達は，ALS2蛋白質が低分子G蛋白質Rab5を基質とするグアニンヌクレオチド交換因子（GEF）活性を有する事，この活性を背景とする神経細胞シグナル伝達にかかわるエンドソーム分子動態にかかわる事を確認した[3)]．さらに，ALS2蛋白質は発現の強弱はみとめられるものの，中枢神経系のみならず組織全体で幅広く発現している．このような現象はALS2蛋白質にかぎらず，ほとんどの遺伝性神経疾患責任遺伝子においても共通している発現パターンである．したがって，神経組織・細胞特異的なALS2蛋白質の機能を保障する共役因子の存在が想定される．一方，神経細胞内でのALS2蛋白質は樹状突起に局在する傾向を示している．したがって，ALS2蛋白質は上記機能を背景とする上位運動ニューロンに特異的な情報伝達あるいは物質輸送や機能維持に深くかかわっていると考えられる．一方，上記の独立した9家系のALS2遺伝子変異に共通したALS2蛋白質機能喪失は，ALS2蛋白質のC-末端に同定されたRab5GEF活性の消失にあると考えられる．

これらの活性調節機能の喪失（たとえば回収できなくなった上位運動ニューロンにユニークなglutamate受容体を介したCaイオンの過剰流入にともなう神経細胞障害）こそがALS2の発症，すなわち上位運動ニューロンをdeath-spiralへと導く最初のでき事であると推定される．

私達はALS2の分子病態解析を目的としてALS2モデル動物の作出を試みた．ALS2蛋白質のほぼ全長を欠失しているTunisiaのALS2家系患者と同一の遺伝子型を持つAls2 *knock-out* (KO) *mouse* を作出した．しかし，当該マウスは生後8カ月を過ぎた時点においても発症していない（他の4研究グループのAls2 KO mouseも発症していない）．上位運動神経変性モデル動物としてマウスの妥当性もうたがわれるが，ALS2遺伝子変異がALS2を始めとしてPLSやHSPの責任遺伝子であることから発症に第2の遺伝子の関与もうたがわれる．これらの可能性については，現在遂行している経時的な神経病理学的解析の結果を待って判定したい．

## ま と め

孤発性，家族性を問わずALSは“heterogeneous group of inexorable neurodegenerative disorders”である．したがって，ALSの発症と進行には複数の因子（遺伝子）の関与が想定される．これら複数の因子を同定し，それらの機能と分子環境を統合して理解する事が運動ニューロン変性の分子機序に基づいた本態治療を可能にする唯一の道である．運動神経の変性に直接あるいは間接的にかかわる因子を的確に把握するためにはALSをはじめ家族性運動神経変性疾患責任遺伝子の単離・同定が必須である．とくに，loss-of-functionをともなう劣性遺伝形式をとる運動神経変性責任遺伝子こそが，遺伝子機能と神経細胞死を直接結びつける格好の因子である．遺伝子同定には，患者，神経内科医，分子医学研究者らの連携，膨大なDNA・遺伝子解析を敢行する努力と継続する意志，それを支えるチームワークと研究費が必要である．私達のALS2遺伝子単離・同定と一連の解析もその例外ではない．ALS2蛋白質の分子動態・機能解析とALS2発症の分子機序の解明を通して，運動ニューロンをふくめた神経細胞系の生存・機能維持の分子基盤の理解を深め，ALSおよび神経変性疾患の本態治療法・治療薬の開発のための新たな展開が拓かれることを期待している．

## 文　献


1) Ben Hamida M, Hentati F, Ben Hamida C : Hereditary motor system diseases (chronic juvenile amyotrophic lateral sclerosis). Brain 1990 ; 113 : 347—363
2) *Rosen DR, Siddique T, Patterson D, et al* : Mutations in Cu/Zn superoxide dismutase gene are associated with familial amyotrophic lateral sclerosis. Nature 1993 ; 362 : 59—62
3) Hadano S, Hand CK, Osuga H, et al : A gene encoding a putative GTPase regulator is mutated in familial amyotrophic lateral sclerosis 2. Nature Genetics 2001 ; 29 : 166—173
4) *Yang Y, Hentati A, Deng HX, et al : The gene encoding* alsin, a protein with three guanine-nucleotide exchange factor domains, is mutated in a form of recessive amyotrophic lateral sclerosis. Nature Genetics 2001 ; 29 : 160—165
5) Eymard-Pierre E, Lesca G, Dollet S, et al : Infantile-onset ascending hereditary spastic paralysis is associated with mutations in the alsin gene. Am J Hum Genet 2002 ; 71 : 518—527
6) Gros-Louise F, Meijer IA, Hand CK, et al : An ALS2 gene mutation causes hereditary spastic paraplegia in a Pakistani kindred. Ann Neurol 2003 ; 53 : 144—145
7) Devon RS, Helm JR, Rouleau GA, et al : The first nonsense mutation in alsin resultes in a homogeneous pheno-

type of infantile-onset ascending spastic paralysis with bulbar involvement in two siblings. Clin Genet 2003；64：210—215

8) Otomo A, Hadano S, Okada T, et al：ALS2, a novel guanine nucleotide exchange factor for the small GTPase Rab5, is implicated in endosomal dynamics. Hum Mol Genet 2003；12：1671—1687

## Abstract

### Recessive motor neuron diseases：Mutations in the ALS2 gene and molecular pathogenesis for the upper motor neurodegeneration

Joh-E Ikeda, Ph.D.
Tokai University, Graduate School of Medicine, Neurodegenerative Diseases Research Centre

We have initially identified a mutation in ALS2 as a causative for a juvenile autosomal recessive form of amyotrophic lateral sclerosis（ALS）, termed ALS2（OMIM 205100）. ALS2 mutations also are causative for an autosomal recessive juvenile primary lateral sclerosis, and infantaile-ascending hereditary spastic paralysis. To date, nine homozygous ALS2 mutaions from nine independent families have been identified. All of these mutations result in predicted premature translation termination caused by the recessive frameshift or nonsense mutation. ALS2 is a 184-kD protein comprising several putative guanine nucleotide exchange factor（GEF）domains [RLD；RCC1 like domain, DH. PH domain, VPS9；Vacuolar protein sorting 9 domain]. In vitro, ALS2 specifically binds to the small GTPase Rab5 and functions as a GEF for Rab5. Ectopic expression of full-length ALS2 has further implied an association with endosomal membranes mediated by the VPS9 domain, consistent with ALS2 involvement in endosomal trafficking and fusion in conjunction with the activation of Rab5. These results combined with our findings suggest that an obstruction of endosomal dynamics might underlie neuronal dysfunction and degeneration in ALS2, PLSJ, and HSP, as well as in a number of other motor neuron diseases.

(Clin Neurol, 44：792—794, 2004)

**Key words**：familial amyotrophic lateral sclerosis；FALS, ALS2 gene, guanine nucleotide exchange factor；GEF, endosomal dynamics

Journal of Cerebral Blood Flow & Metabolism (2005), 1–13

www.jcbfm.com

# A dopamine D4 receptor antagonist attenuates ischemia-induced neuronal cell damage via upregulation of neuronal apoptosis inhibitory protein

Yoshinori Okada[1,2], Harumi Sakai[1], Eri Kohiki[3], Etsuko Suga[3], Yoshiko Yanagisawa[3], Kazunori Tanaka[1], Shinji Hadano[1,3], Hitoshi Osuga[1,3] and Joh-E Ikeda[1,3,4]

[1]*Department of Molecular Neuroscience, The Institute of Medical Sciences, Tokai University, Isehara, Kanagawa, Japan;* [2]*Laboratory for Structure and Function Research, Tokai University School of Medicine, Isehara, Kanagawa, Japan;* [3]*Solution Oriented Research for Science and Technology (SORST), Japan Science and Technology Agency (JST), Tokai University School of Medicine, Isehara, Kanagawa, Japan;* [4]*Department of Paediatrics, University of Ottawa, Ottawa, Ontario, Canada*

**Neuronal apoptosis inhibitory protein (NAIP/BIRC1), the inhibitor of apoptosis protein (IAP) family member, suppresses neuronal cell death induced by a variety of insults, including cell death from ischemia and stroke. The goal of the present study was to develop an efficient method for identification of compounds with the ability to upregulate endogenous NAIP and to determine the effects on these compounds on the cellular response to ischemia. A novel NAIP-enzyme-linked immunosorbent assay (ELISA)-based *in vitro* drug-screening system is established. Use of this system identified an antagonist of dopamine D4 receptor, termed L-745,870, with a potent NAIP upregulatory effect. L-745,870-mediated NAIP upregulation in neuronal and nonneuronal cultured cells resulted in decreased vulnerability to oxidative stress-induced apoptosis. Reducing NAIP expression via RNA interference techniques resulted in prevention of L-745,870-mediated protection from oxidative stress. Further, systemic administration of L-745,870 attenuated ischemia-induced damage of the hippocampal CA1 neurons and upregulated NAIP expression in the rescued hippocampal CA1 neurons in a gerbil model. These data suggest that the NAIP upregulating compound, L-745,870, has therapeutic potential in acute ischemic disorders and that our NAIP-ELISA-based drug screening may facilitate the discovery of novel neuroprotective compounds.**
*Journal of Cerebral Blood Flow & Metabolism* advance online publication, 23 February 2005; doi:10.1038/sj.jcbfm.9600078

**Keywords:** antiapoptosis; dopamine receptor antagonist; IAP; ischemia; NAIP; oxidative stress

## Introduction

Several studies have demonstrated that the mechanisms of ischemia-induced neuronal cell death fall on the continuum between necrosis and apoptosis (Raghupathi *et al*, 2000; Graham and Chen, 2001). While relatively more interest has been focused on prevention of cell necrosis after ischemic insults, apoptosis, with its ordered series of events, including caspase activation (Graham and Chen, 2001) and/or the perturbation of calcium homeostasis (Love, 1999), may represent a more suitable target for modulation for the goal of preventing cell death. This may be particularly true for neuronal damage after cerebral ischemia (Nitatori *et al*, 1995).

Recent studies have demonstrated that various antiapoptotic proteins, including Bcl-2, neuronal apoptosis inhibitory protein (NAIP, also called baculoviral IAP repeat-containing 1 (BIRC1)), and X-linked inhibitor of apoptosis (XIAP), are upregulated in neurons after ischemia (Graham and Chen, 2001; Krajewski *et al*, 1995; Xu *et al*, 1997, 1999). Among these antiapoptotic proteins, NAIP, the founding member of the inhibitor of apoptosis protein (IAP) family, was identified in the course

Correspondence: Dr J-E Ikeda, Department of Molecular Neuroscience, The Institute of Medical Sciences, Tokai University, Isehara, Kanagawa 259-1193, Japan.
E-mail: jei@m.med.u-tokai.ac.jp
This work was funded by the Japan Science and Technology Agency (JST). A part of the work was supported by a Grant-in-Aid for Scientific Research on Priority(C)-Advanced Brain Science Project from the Ministry of Education, Culture, Sports, Science, and Technology of Japan.
Received 4 August 2004; revised 15 November 2004; accepted 6 December 2004

of the positional cloning of the gene responsible for spinal muscular atrophy (SMA) (Roy *et al*, 1995). In actuality, the primary genetic defect in SMA results from mutations in an adjacent gene, survival motor neurons (SMN). However, patients with the most severe form of SMA have large deletions that encompass both the *SMN* and *NAIP* genes. These data suggest that NAIP may also play a role in neuronal viability (Gavrilov *et al*, 1998; Hsieh-Li *et al*, 2000; Monani *et al*, 2000).

Indeed, overexpression of NAIP by adenovirus-mediated gene transfer reduces ischemic cell damage in the rat hippocampus (Xu *et al*, 1997). Further, ectopic NAIP expression rescues motor neurons after peripheral nerve axotomy (Perrelet *et al*, 2000) and preserves nigrostriatal dopaminergic function in the intrastriatal 6-hydroxydopamine (6-OHDA) rat model of Parkinson's disease (Crocker *et al*, 2001). Moreover, NAIP promotes motor neuron survival through the intracellular signaling of glial cell-derived neurotrophic factor (GDNF) (Perrelet *et al*, 2002). Finally, unlike other IAP proteins and Bcl-2 family proteins, NAIP exerts a unique antiapoptotic activity against oxidative stresses. These findings suggest that NAIP plays an important role in the protection of the neuronal cells from apoptotic insults, and that upregulation of endogenous NAIP may represent a therapeutic approach for prevention of oxidative stress-induced neuronal cell damage.

Therefore, the goal of the present study was to develop an efficient method for identification of compounds with the ability to upregulate endogenous NAIP and to determine the effects of these compounds on the cellular response to ischemia.

## Materials and methods

### Chemicals

A total of 953 compounds, including 3-[(4-[4-chlorophenyl]piperazine-1-yl)methyl]-[1H]-pyrrolo[2,3-*b*] pyridine-trihydrochloride (L-745,870) listed in 'Neurochemicals, Signal Transduction Agents, Pharmacological Probes and Biochemicals compounds; Tocris Cookson Ltd', was purchased from Tocris Cookson Ltd (Bristol, UK) and subjected to drug-screening experiments. Drug concentrations were tested in a range from 1 to 100 μmol/L. All other cytotoxins including menadione, $H_2O_2$, α-naphthoquinone, 2,3-dimethoxy-1,4-naphthoquinone (DMNQ), actinomycin D, staurosporine, *cis*-platinum, okadaic acid, oligomycin, and etoposide were purchased from Sigma-Aldrich (St Louis, MO, USA).

### Antibodies

Two independent anti-human NAIP antibodies, IB9 and ME1, were generated. IB9, a mouse monoclonal antibody, was raised using an epitope of the human NAIP C-terminal peptide (amino acids 841 to 1052), and a polyclonal antibody, ME1 (1:3,000 dilution), was obtained by immunizing rabbits with recombinant NAIP peptide (amino acids 256 to 587). ME1 recognizes the BIR3 region of NAIP and crossreacts with the mouse and gerbil NAIP proteins (data not shown). Other antibodies used in this study included rabbit polyclonal anti-XIAP antibody (#AF822; 1:1,000; R&D Systems, Minneapolis, MN, USA), rabbit polyclonal anti-cIAP-1 antibody (#AF818; 1:1,000; R&D Systems), rabbit polyclonal anti-cIAP-2 antibody (#AF817; 1:1,000; R&D Systems), rabbit polyclonal anti-Survivin antibody (#NB500-201; 1:1,000; Novus Biologicals, Littleton, CO, USA), rabbit polyclonal anti-Bcl-2 antibody (#SC-783; 1:1,000; Santa Cruz Biotechnology, CA, USA), rabbit polyclonal anti-Bcl-xL antibody (#SC-634; 1:1,000; Santa Cruz Biotechnology), and mouse monoclonal anti-β-tubulin antibody (#SC-5274; 1:50,000; Santa Cruz Biotechnology).

### Cell Lines and Culture Conditions

The human monocyte-derived cell line, THP-1, was cultured in RPMI-1640 (Invitrogen, Carlsbad, CA, USA), while HeLa and SH-SY5Y neuroblastoma cells were cultured in Dulbecco's modified Eagle's medium (DMEM) (Invitrogen). All culture media contained penicillin (50 IU/mL) and streptomycin (50 μg/mL) and were supplemented with 10% fetal calf serum. SH-SY5Y cells, which were seeded with a density of $4 \times 10^5$ cells/well in six-well plates, were differentiated by treatment with all-*trans*-retinoic acid (Tocris Cookson) at a concentration of 10 μmol/L.

### NAIP-ELISA and Screening of NAIP Upregulating Compounds

NAIP-neuronal apoptosis inhibitory protein-enzyme-linked immunosorbent assay (ELISA)-based screening with THP-1 cells was conducted to identify compounds that induced endogenous NAIP expression. THP-1 cells were cultured in 24-well plates at a density of $2 \times 10^5$ cells/well for 24 h, followed by incubation in the presence of tested compounds for either 24 or 72 h. Cells were then lysed with NP40 buffer (50 mmol/L Tris-HCl, pH 7.5, 150 mmol/L NaCl, 1% NP40, and protein inhibitor cocktail (Complete; Roche Diagnostics, Indianapolis, IN, USA)). Aliquots of extracts were subjected to the NAIP-ELISA assay, with 1B9 as primary antibody conjugated to the ELISA plate and with ME1 as secondary antibody for quantification of NAIP immunoreactivity. Assays were conducted according to standard ELISA procedure (Crowther, 1995).

### Western Blot Analysis

The extracts from cultured cells were electrophoretically separated on 5% to 20% SDS-polyacrylamide gels and transferred onto polyvinylidene difluoride (PVDF) membranes (Bio-Rad Laboratories, Hercules, CA, USA). Membranes were then incubated with the indicated primary antibodies in TBST buffer (50 mmol/L Tris-HCl; pH 7.4, 150 mmol/L NaCl, 0.1% (w/v) Tween-20) for 2 h, after

incubation with the peroxidase-linked secondary anti-rabbit IgG (#NA934; Amersham Pharmacia Biotech, Uppsala, Sweden) or anti-mouse IgG (#NA931; Amersham Pharmacia Biotech) antibody for 1 h. Signals were detected using ECL Plus (Amersham Pharmacia Biotech).

### Cell Viability Assay

Approximately $1 \times 10^5$ cells, which were either pretreated with 10 μmol/L of L-745,870 for 24 h or left untreated, were plated on a 96-well plate and incubated for 5 h at 37°C. The appropriate amounts of the cytotoxins, including free radical generating compounds (DMNQ: 120 μmol/L, menadione: 20 to 80 μmol/L, α-naphthoquinone: 60 μmol/L and $H_2O_2$: 30 μmol/L), kinase inhibitor (staurosporine: 1 nmol/L), ATPase inhibitor (oligomycin: 100 μmol/L), DNA-damaging reagent (*cis*-platinum: 100 μmol/L), phosphatase inhibitor (okadaic acid: 100 nmol/L), and topoisomerase II inhibitors (actinomycin D: 1 μmol /L and etoposide: 100 μmol/L), were added, and the preparation was allowed to incubate for another 1 to 10 h. The medium was then replaced with fresh medium containing 10% (v/v) alamarBlue (AccuMed International, Westlake, OH, USA), followed by incubation for an additional 4 h at 37°C. Cell numbers were counted fluorometrically as per the alamarBlue Assay instructions.

### Flow-Cytometric Analysis of Apoptotic/Necrotic Cell Death

Quantification of the apoptotic/necrotic cell death was performed by flow cytometry in conjunction with the MEBCYTO Apoptosis Kit (MBL, Nagoya, Japan). In brief, HeLa cells that were pretreated with or without L-745,870 were plated on a six-well plate ($3 \times 10^5$ cells/well). After 4 h of incubation, menadione (or $H_2O_2$) was added to the cells, followed by incubation for an additional 4 h (or 40 mins for $H_2O_2$). The cells were washed once with phosphate-buffered saline (PBS) and suspended in fresh medium for Annexin V-FITC and propidium iodide (PI) labeling, which was performed according to the manufacturer's instructions (MBL). The cells were sorted and analyzed by FACScan (Beckton Dickinson, San Jose, CA, USA). Cell damage was classified according to the extent of staining of AnnexinV-FITC and PI (Quadrant analysis). Quadrants were comprised of the upper left (UL; AnnexinV−/PI+), upper right (UR; AnnexinV+/PI+), low left (LL; AnnexinV−/PI−), and low right (LR; AnnexinV+/PI−). LL, LR, and UR represent the cells in normal state, early stage of apoptosis, and late stage of apoptosis/necrosis, respectively.

### RNA Interference

Neuronal apoptosis inhibitory protein RNA interference (RNAi) was achieved by expressing the hairpin-forming short RNA molecules generated from a portion of the 3′UTR of the human *NAIP/BIRC1* gene. Briefly, 19-nucleotide-long inverted repeats, 5′-GTCAACTCCCCTCCCCTTG-3′ (sense) and 5′-CAAGGGGAGGGGAGTTGAC-3′ (antisense), which were intervened with the 9-nucleotide spacer (TTCAAGAGA), were inserted downstream of the U6 promoter of pSilencer 1.0-U6 vector (Ambion, Austin, TX, USA), generating pSilencer 1.0-U6-NAIP. HeLa cells, which were either pretreated with L-745,870 for 24 h or left untreated, were cotransfected with 10 μg of pSilencer 1.0-U6-NAIP and 1 μg of pMACS $K^k$.II (Miltenyi Biotec, Bergisch Gladbach, Germany) using FuGENE6 (Roche Diagnostics). After 48 h, the transfected cells were magnetically enriched and cultured for 24 h. NAIP expression and cell viability were analyzed by Western blotting and by the alamarBlue Assay, respectively.

### Generation of Forebrain Ischemic Model in Gerbils

All animal experimental procedures were performed in accordance with the guidelines of the Tokai University School of Medicine Committee on Animal Care and Use. Twelve-week-old Male Mongolian gerbils (Clea Japan Inc., Tokyo, Japan), weighing 70 to 80 g, were used. Animals were anesthetized with halothane (4%) in a mixture of $N_2O/O_2$ (70:30) initially, and halothane was gradually decreased to 2% for maintenance of anesthesia during surgery. Under anesthesia, a femoral artery catheter was placed to monitor mean arterial blood pressure, and rectal and temporal muscle temperatures were monitored and maintained at 37°C±0.5°C via a heating pad and radiant heat during and after surgery. Forebrain ischemia was induced by bilateral common carotid artery occlusion (BCCAO) using 3-mm sugita-aneurysm clips (Kirino and Sano, 1984). After 10 mins of occlusion, the aneurysmal clips were removed to allow reperfusion, and complete reperfusion of the arteries was verified by direct visual observation. Sham-operated gerbils underwent identical surgery with the exception of the BCCAO procedure. Under these experimental conditions, in which a relatively severe ischemic condition was used, all animals survived until fixation.

To investigate the *in vivo* effect of L-745,870 (Tocris Cookson Ltd) on ischemia-induced cell death, the compound was dissolved in physiologic saline and was administered to gerbils at a dose of 7 mg/kg ($n=6$), 70 mg/kg ($n=7$), 140 mg/kg ($n=7$), or 210 mg/kg ($n=6$). We have administered the compound to the animals 1 h before ischemic surgery to ensure the protection of neurons from the oxidative stress-induced cell death. This experimental protocol was designed based on the *in vitro* experimental data in which the pretreatment with the compound effectively protects cultured cells from the menadione-induced insults (refer to Figures 1 to 4). Administration of the compound was performed intragastrically via oral cannula under anesthesia. Vehicle-treated animals ($n=7$) received physiologic saline alone. Sham-operated animals ($n=3$) were administered with a compound dose of 210 mg/kg.

### Measurement of Regional Cerebral Blood Flow

To analyze the effect of the compound on regional cerebral blood flow (CBF), a subset of animals underwent measure-

ment of CBF at 2 and 24 h after administration of L-745,870 (210 mg/kg) or vehicle. Cerebral blood flow was measured by the hydrogen clearance method via a platinum wire electrode stereotaxically inserted into the right hippocampus using coordinates of 2 mm posterior and 2 mm lateral to the bregma, and 2.5 mm below the brain surface in a flat cranial presentation, as previously reported (Osuga *et al*, 2000).

### Histopathology

After 3 days of reperfusion, animals were anesthetized with 4% halothane and perfused with 60 mL of 4% paraformaldehyde in phosphate buffer (pH 7.4) via a catheter placed in the heart. The brains were removed, fixed in 10% formalin for 10 days, and embedded in paraffin. Paraffin sections were sliced at a thickness of 7 $\mu$m for histopathologic and immunohistochemical evaluation. Neuronal cell density of the CA1 subfield of the hippocampus, that is, the number of intact CA1 pyramidal neurons per 1 mm linear length of pyramidal cell layer, was measured by counting 7 $\mu$m sections stained with hematoxylin and eosin from 3 to 7 independent animals in a double-masked manner.

### Immunohistochemistry

Brain sections were subjected to NAIP and XIAP immunohistochemistry with polyclonal anti-human NAIP (ME1) and XIAP antibodies (R&D Systems Inc.), respectively, and stained using the Vectastain elite ABC kit (Vector Laboratories Inc., Burlingame, CA, USA) according to the manufacturer's instructions. In brief, after deparaffinization, the sections were washed with 0.01 mol/L PBS (pH 7.2) for 5 mins and were incubated with anti-NAIP (5 $\mu$g/mL) or anti-XIAP (5 $\mu$g/mL) antibody overnight at 4°C. The sections were rinsed three times with PBS containing 0.05% Triton X-100 for 10 mins, incubated with biotinylated secondary antibody for 3 h, and then incubated with avidin–biotin–peroxidase complex for 1 h at room temperature. Finally, the sections were treated with 0.5% 3,3′-diaminogenzidine (DAB) and 0.01% $H_2O_2$ in Tris-HCl buffer (pH 7.5), and the DAB reaction products were observed under a microscope.

### Statistical Analysis

All data in this study are presented as mean ± s.e. Data were analyzed for significance using Student's *t*-test for pair-wised comparisons or ANOVA followed by Scheffe's test for multiple comparisons between groups (Statview 5.0 software; SAS, Cary, NC, USA). A *P*-value $<0.05$ was considered as reaching statistical significance.

## Results

### Identification of NAIP Upregulating Compounds

To identify compounds with the ability to induce NAIP expression, 953 compounds (Tocris) were screened using NAIP-ELISA. Compounds were arbitrarily categorized as 'downregulator' ($n=16$) if the resulting NAIP level was less than 70% of the normal endogenous level (i.e., ~12 ng/mL), or 'upregulator' ($n=30$) if the resulting NAIP level was more than 200% of the normal endogenous NAIP level (Table 1).

To examine whether the 30 identified NAIP upregulators suppressed menadione-induced cell death, THP-1 cell viability assays were performed in cells pretreated with menadione followed by the addition of each NAIP upregulator. All 30 compounds exerted a protective effect against menadione-induced cell death with variable degrees (Table 1). The compound that exerted the most potent protective effect was L-745,870, a dopamine D4 receptor antagonist (Figure 1A). This compound was used for subsequent experiments.

### L-745,870 Protects a Variety of Cultured-Cells Against Menadione-Induced Cell Death

To determine whether the protective effect of L-745,870 on THP-1 cells was specific to cell type, cell viability studies were also conducted in HeLa and SH-SY5Y (differentiated neuroblastoma by all-*trans*-retinoic acid treatment) cells after exposure to the compound. L-745,870 protected both cell lines from menadione-induced cell death (Figures 1A, THP-1; B, HeLa; and C, SH-SY5Y). Further, the dose-

**Table 1** Screening of 953 Tocris compounds by NAIP-ELISA, and viability assays after challenging with menadione-induced oxidative stress in THP-1 cells

| *NAIP level* | *NAIP concentration* | | | *Cell viability (%)* |
|---|---|---|---|---|
| | *Mean ± s.e. (ng/mL)* | *Minimum (ng/mL)* | *Maximum (ng/mL)* | *(n) (menadione; 40 μmol/L)* |
| Untreated (control) | 12.4 ± 0.3 (240) | 11.8 | 12.7 | 31–37% (30) |
| *Compound* treated | | | | |
| Unchanged | 12.9 ± 0.4 (907) | 10.1 | 21.3 | ND* |
| Upregulator | 54.8 ± 12.1 (30) | 31.8 | 78.8 | 45–93% (30) |
| Downregulator | 8.6 ± 0.8 (16) | 7.1 | 9.1 | ND* |

NAIP, neuronal apoptosis inhibitory protein; ELISA, enzyme-linked immunosorbent assay; *ND, not determined. Number in each parenthesis indicates the number of tested compounds.

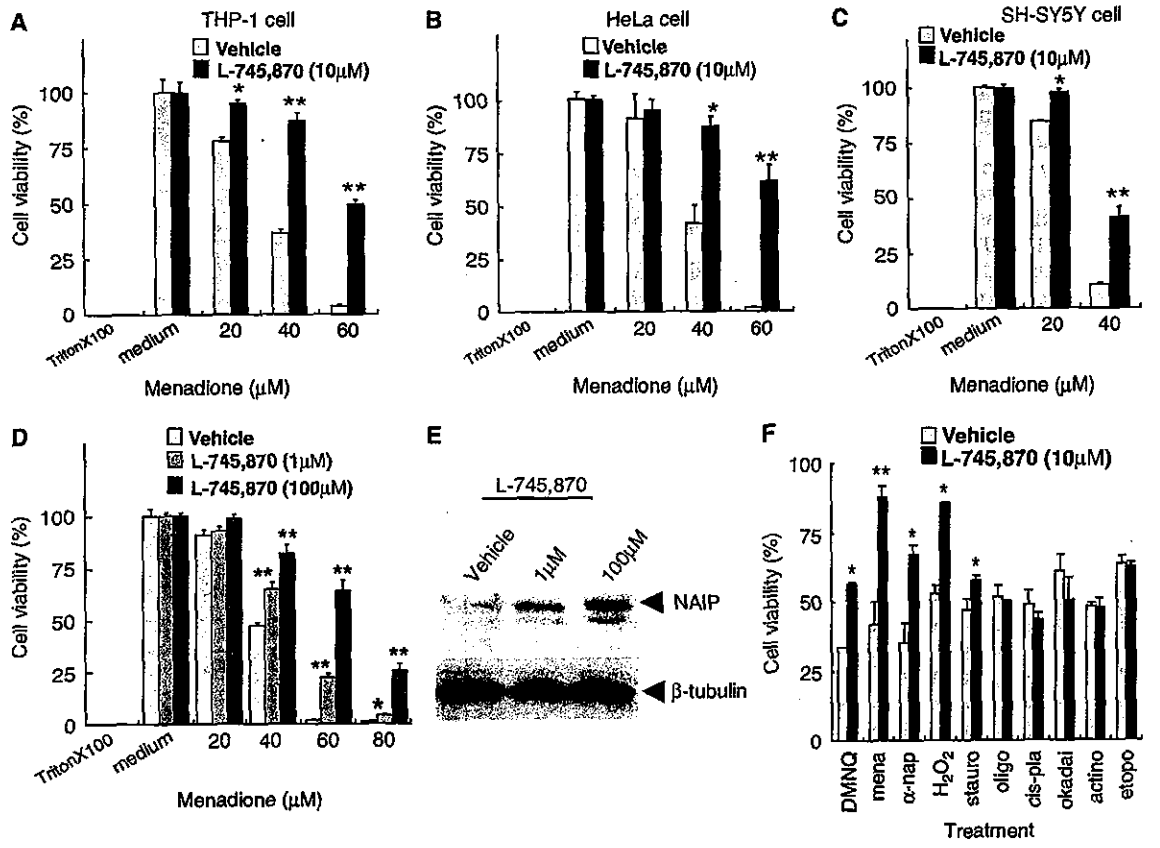


**Figure 1** The effect of L-745,870 on oxidative stress-induced cell death. Cell viability after menadione treatment in (**A**) THP-1, (**B**) HeLa, and (**C**) differentiated SH-SY5Y cells was assayed. Cells that were pretreated with vehicle or L-745,870 (10 μmol/L) for 24 h were challenged with menadione (0 to 100 μmol/L) for 4 h. Each value represents the percentages of the cell viability relative to those of control (Triton X-100-treated cells) (means ± s.e.; $n = 8$). $^{*}P < 0.01$; $^{**}P < 0.001$, versus each corresponding vehicle. Statistical analysis was performed using Student's *t*-test. (**D** and **E**) Effect of various concentrations of L-745,870 on neuronal apoptosis inhibitory protein (NAIP) expression and cell viability after menadione treatment in HeLa cells. (**D**) Cells were pretreated with vehicle or L-745,870 (1 and 100 μmol/L) for 24 h and then challenged with menadione (0 to 100 μmol/L) for 4 h. $^{*}P < 0.01$; $^{**}P < 0.001$, versus each corresponding vehicle. Statistical analysis was performed using ANOVA with Scheffe's *post hoc* test. (**E**) Western blotting analysis of NAIP in HeLa cells treated with L-745,870 (1 and 100 μmol/L) or vehicle for 24 h. The arrowhead indicates the position of NAIP (150 kDa). Expression of β-tubulin was not affected by L-745,870 treatment and shows that equal amount of proteins loaded in each lane of the blot. (**F**) Effects of L-745,870 on cell viability after exposure to cell death-inducing agents in HeLa cells. Cells were pretreated with vehicle or L-745,870 (10 μmol/L) for 24 h and then exposed to various reagents, including DMNQ, menadione (mena), α-naphthoquinone (α-na), $H_2O_2$, staurosporine (stauro), oligomycin (oligo), *cis*-platinum (*cis*-pla), okadaic acid (okadaic), actinomycin D (actino), and etoposide (etopo). $^{*}P < 0.01$; $^{**}P < 0.001$, versus each corresponding vehicle. Statistical analysis was performed using Student's *t*-test.

dependent increase in cell viability correlated with a concomitant increase in NAIP level in HeLa cells (Figures 1D and 1E).

### L-745,870 Selectively Protects Cells Against Oxidative Stress-Induced Apoptosis

To gain insight into the suppression of the cell death with L-745,870, HeLa cells pretreated with L-745,870 were challenged with various apoptosis-inducing stimuli and chemical cell-stressors. L-745,870 specifically suppressed cell death induced by oxidative stressors, including cell death in response to menadione, hydrogen peroxide ($H_2O_2$), DMNQ, and α-naphthoquinone, but did not protect against cell death induced by nonoxidative stressors (e.g., staurosporine, oligomycin, *cis*-platinum, okadaic acid, actinomycin D, and etoposide) (Figure 1F).

To confirm the antiapoptotic effect of L-745,870 against oxidative stress-induced cell death, flow cytometric analysis of cell treated with L-745,870 and menadione and double-stained with Annexin V-FITC and PI was performed. Half of the population of the menadione-treated cells that were not